1301

Université de Neuchâtel
Faculté des Sciences

Le modèle XY classique: frustration, modulation et réseau fractal

Forme réduite de la thèse présentée par

André Vallat

Ingénieur physicien diplômé
de l'Ecole Polytechnique Fédérale de Lausanne
pour l'obtention du grade de docteur ès sciences
de l'Université de Neuchâtel

Institut de Physique
Université de Neuchâtel

Mai 1991

IMPRIMATUR POUR LA THÈSE

Le modèle XY classique : Frustration, modulation et réseau fractal.

de M. André Vallat

UNIVERSITÉ DE NEUCHÂTEL

FACULTÉ DES SCIENCES

La Faculté des sciences de l'Université de Neuchâtel sur le rapport des membres du jury,

Messieurs H. Beck, P. Martinoli,
Ph. Choquard (Lausanne) et J. Villain (Grenoble).

autorise l'impression de la présente thèse.

Neuchâtel, le 13 juin 1996

Le doyen:

R. Dändliker

La thèse complète a été déposée
à l'Institut de Physique
de l'Université de Neuchâtel

et les publications ci-jointes en
représentent l'essentiel:

- "XY model on a Sierpinski gasket." A. Vallat, S.E. Korshunov et H. Beck, Phys. Rev. B **43**, 8482 (1991).
- "Classical frustrated XY model: Continuity of the ground state energy as a function of the frustration." A. Vallat et H. Beck, Phys. Rev. Lett. **68**, 3096 (1992).
- "Coulomb gas representation of the two-dimensional XY model on a torus." A. Vallat et H. Beck, Phys. Rev. B **50**, 4015 (1994).
- "Frustrated XY models with accidental degeneracy of the ground state." S.E. Korshunov, A. Vallat et H. Beck, Phys. Rev. B **51**, 3071 (1995).

XY model on a Sierpinski gasket

A. Vallat
Institut de Physique, Université Neuchâtel, Breguet 1, CH-2000 Neuchâtel, Switzerland

S. E. Korshunov
L. D. Landau Institute for Theoretical Physics, Kosygina, 2, 117334 Moscow, USSR

H. Beck
Institut de Physique, Université de Neuchâtel, Breguet 1, CH-2000 Neuchâtel, Switzerland

(Received 6 August 1990)

Correlation functions and topological excitations of the XY model on a Sierpinski gasket are studied. The energy of a vortex is shown to be finite, so no Berezinskii-Kosterlitz-Thouless transition can be expected to take place. At any temperature the correlation function decays exponentially at large distances. A form of the XY model on a Sierpinski gasket is found that allows for exact renormalization. The results obtained can be applied to superconducting wire networks and tunnel-junction arrays.

I. INTRODUCTION

Recent progress in the techniques of lithography has led to the development of an interesting branch of experimental physics, namely, the fabrication and investigation of two-dimensional superconducting systems (tunnel-junction arrays and wire networks) with different regular or irregular structures.[1] This means that one has the possibility to produce quasicrystalline, fractal, or some other nontrivial superconductors. For example, wire networks in the form of a Sierpinski gasket have been studied by Gordon *et al.* [2] and more recently by Martinoli *et al.* [3]

On the other hand theoretical investigations of fractal superconducting wire networks have not, so far, gone beyond the application of the Landau-Ginzburg approximation.[4,5] Such an approach is certainly not sufficient, since even in two dimensions the phase fluctuations of the superconducting order parameter are very important both for the properties of the ordered phase and for the phase transition. In the case of a Sierpinski gasket with effective dimensionality less than two one can expect them to be of even greater importance.

In this paper we investigate the influence of the fluctuations on the properties of a fractal superconducting system on the example of the Sierpinski gasket (Fig. 1). When only the most relevant phase fluctuations are taken into account, the 2D-superconducting system can be described by one or another type of XY model. The Josephson junction array, for example, will be described by the ordinary XY model with cosine interaction

$$H=-J\sum_{\langle r,r'\rangle}\cos(\theta_r-\theta_{r'})\ , \tag{1}$$

where variables θ_r's stand for the phases of the order parameter of corresponding superconducting grains. The summation in Eq. (1) is taken over pairs of nearest neighbors on a lattice that are connected by Josephson junctions.

On the other hand the phase fluctuations in the wire network should be described by the Hamiltonian

$$H=\int dl\frac{J_0}{2}\left[\frac{\partial\theta}{\partial l}\right]^2, \tag{2}$$

where integration should be performed over the whole network bearing in mind that θ is a multivalued function. Hamiltonian (2) being quadratic in θ, one can integrate out from the corresponding partition function the fluctuations of θ on the wires but not on the nodes of the network, obtaining in such a way

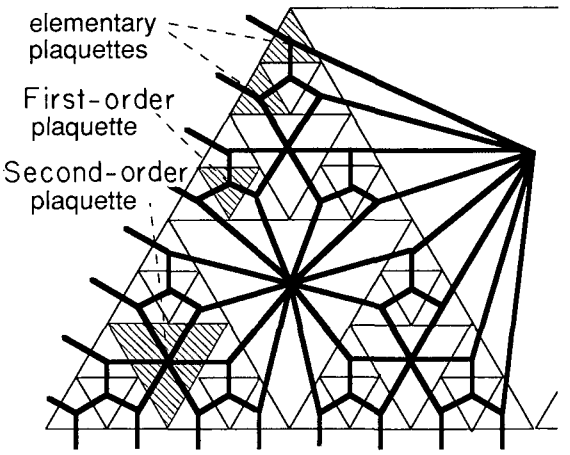

FIG. 1. The Sierpinski gasket is constructed with elementary triangles (or elementary plaquettes). The first-order fractal is formed by combining three of them. In the general case the $(s+1)$-order fractal is obtained by the juxtaposition of three s-order fractals. We will call the greatest plaquette which is situated in the center of s-order fractal an s-order plaquette, and sites at its three corners the s-order sites. The dual lattice is shown in bold lines. Each bond of a dual lattice intersects a bond of a direct lattice.

$$Z=\sum_{\{m_{rr'}\}}\exp\left[-\frac{K}{2}\sum_{\langle r,r'\rangle}(\theta_{r'}-\theta_r-2\pi m_{rr'})^2\right],$$
$$K=\frac{J}{k_BT},\quad J=\frac{J_0}{L}, \tag{3}$$

where θ_r stands for the values of θ at the nodes of the network and m is the winding number. In the general case J would be dependent on the length L of the link, but we will be interested only in the case of all links being of equal length. The partition function of the form (3) corresponds to an interaction between θ_r and $\theta_{r'}$ that is very close to a cosine function for $K\ll 1$ and to a piecewise parabolic function for $K\gg 1$. The interaction incorporated in Eq. (3) was initially introduced by Berezinskii[6] and Villain[7] instead of a cosine for the sake of convenience, because it allows for a number of various rigorous transformations to other representations. We would like to emphasize here that for a network (in contrast to an array) this particular form of the interaction is the most adequate.

We start our investigation of the XY model on a Sierpinski gasket by developing the harmonic approximation in Sec. II. Then we turn to the investigation of topological excitations (vortices) in Sec. III and finally find a kind of description that explicitly incorporates the periodicity of the phase in Sec. IV. Our main conclusion is that in such models there is no phase transition in the rigorous sense of the word. For arbitrarily low temperature the energy of the vortices is finite and the correlation functions decay exponentially at large enough distances. So in such a system there will be no global phase coherence.

II. HARMONIC APPROXIMATION

In the harmonic approximation any XY model will be described by the Hamiltonian

$$H=\frac{J}{2}\sum_{\langle rr'\rangle}(\theta_r-\theta_{r'})^2=\frac{k_BT}{2}\sum_{r,r'}\theta_r U_{rr'}\theta_{r'}, \tag{4}$$

where the elements of the dimensionless interaction matrix $U_{rr'}$ are equal to $4K$ for $\mathbf{r}=\mathbf{r}'$, to $-K$ for $\mathbf{r}$ and $\mathbf{r}'$ being the nearest neighbors and to 0 elsewhere. The correlation function $g_{rr'}$ will then be determined by the reciprocal matrix $G_{rr'}=(U^{-1})_{rr'}$:

$$\begin{aligned}g_{rr'}&\equiv\langle\exp[i(\theta_r-\theta_{r'})]\rangle\\&=\exp[-\tfrac{1}{2}\langle(\theta_r-\theta_{r'})^2\rangle]\\&=\exp(-\tfrac{1}{2}F_{rr'})\end{aligned} \tag{5}$$

with

$$F_{rr'}\equiv G_{rr}-G_{rr'}-G_{r'r}+G_{r'r'}. \tag{6}$$

$G_{rr'}$ is proportional to the lattice Green function of the Sierpinski gasket. To calculate $G_{rr'}$, it is convenient to express it as

$$G_{rr'}=-\left[\frac{\partial}{\partial h_r}\frac{\partial}{\partial h_{r'}}\ln Z\{h\}\right]_{h=0}, \tag{7}$$

where $Z\{h\}$ stands for the generating function

$$Z\{h\}\equiv\prod_r\left[\int_{-\infty}^{\infty}\frac{d\theta_r}{2\pi}\right]\exp\left[-\frac{K}{2}\sum_{\langle r,r\rangle}(\theta_r-\theta_{r'})^2+i\sum_r h_r\theta_r\right] \tag{8}$$

which for $h=0$ coincides with the partition function Z.

The fractal structure of the Sierpinski gasket allows us to calculate $Z\{h\}$ (and consequently $G_{rr'}$) step by step, by integrating out to the sth step the variables that are defined on the corner sites of the sth order plaquettes of the initial lattice (we shall call such sites the sth order sites, see Fig. 1). For example, after the first integration one obtains

$$Z\{h\}=A_1V_1\{h\}Z_1\{h\}, \tag{9}$$

where A_1 is the numerical factor depending on K, which is irrelevant for calculating G, and $Z_1\{h\}$ has the same structure as $Z\{h\}$:

$$Z_1\{h\}=\prod_r\left[\int_{-\infty}^{\infty}\frac{d\theta_r}{2\pi}\right]\exp\left[-\frac{K_1}{2}\sum_{\langle rr'\rangle}(\theta_r-\theta_{r'})^2+i\sum_r h'_r\theta_r\right] \tag{10}$$

but with a renormalized value of the coupling constant $K_1=(\frac{3}{5})K$ and the variables defined on the decimated lattice. Due to the property of self-similarity, the decimated lattice is again the Sierpinski gasket. In the process of integration, each field h_r defined on the first-order sites splits into three nonequal parts, which are shifted to the neighboring sites of larger order (see Fig. 2), so h' in Eq. (10) stands for the

$$h_r+\sum_{r'}\gamma_{rr'}h_{r'}, \tag{11}$$

where $\gamma_{rr'}=\frac{1}{5}$ or $\frac{2}{5}$ and the sum is taken over six nearest first-order sites.

The exponent of the factor

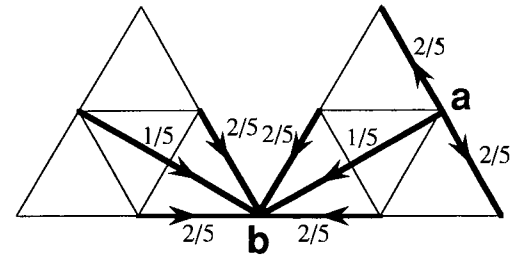

FIG. 2. Illustration of the "splitting" of h_a at the first-order site a. At the superior order site b, all contributions from all first-order sites to h_b are shown.

$$V_1\{h\}=\exp\left[-\frac{1}{20K}\sum(h_{r_1}^2+h_{r_2}^2+h_{r_3}^2+3h_{r_1}h_{r_2}+3h_{r_2}h_{r_3}+3h_{r_3}h_{r_1})\right], \tag{12}$$

where the summation is to be taken over all first order plaquettes and r_α ($\alpha=1,2,3$) are the sites at their corners, gives the first contribution to $G_{rr'}$.

One can repeat the decimation procedure again and again. At each step the structure of $Z_s\{h\}$ is conserved, but the coupling constant is scaled by the factor of $\frac{3}{5}$ and a new additive contribution to $G_{rr'}$ appears of the same form as the exponent in Eq. (12). The series for $G_{rr'}$ turns out to be divergent, but for the combination (6) entering the correlation function (5), it either has a finite number of terms or it is convergent. Unfortunately it is impossible to sum this series analytically.

One can understand how the correlation function decays by considering it for, say, sites r' and r'' which are of the s'th and s'th orders, respectively. Thus one can perform the renormalization procedure for $s=\min\{s',s''\}-1$ times, obtaining the expression for the correlation function for the model [see Eqs. (5)–(8)] with $K_R=(\frac{3}{5})^s K$ with distance r between points equal to $(\frac{1}{2})^s|r'-r''|$. This shows that the correlation function $g(r)$ decays as

$$g(r)\propto\exp\left[-\frac{(\frac{5}{3})^s}{C}\right]\equiv\exp\left[-\frac{r^\nu}{C}\right], \qquad \nu=\frac{\ln(\frac{5}{3})}{\ln 2}, \quad C\propto K\ . \tag{13}$$

Such a law of the decay of the correlation function signifies that there is no quasi-long-range order in the system. But since we are in the harmonic approximation this means that for the fractal network one can have no hope to have a better phase coherence than to have $g(r)$ of the form (13) with $\nu<1$. However there still remains a possibility to have a phase transition into a state with a more rapid decay of $g(r)$.

III. VORTICES

The unrestricted decrease of the coupling constant in the process of the renormalization suggests that for any temperature the harmonic approximation will not be applicable at large enough scales ($d\geq\xi\equiv K^{1/\nu}$). For XY model this usually means that one should also take vortices into consideration. It can be most easily done for the partition function (2) which allows exact decomposition into spin-wave part and vortex part:[8]

$$Z_{XY}=Z_{SW}Z_{vort} \tag{14}$$

with Z_{SW} coinciding in the form with the partition function of the harmonic approximation and

$$Z_{vort}=\sum_{\{n_u\}}\exp\left[-\tfrac{1}{2}\sum_{u,u'}n_u\tilde{G}_{uu'}n_{u'}\right], \tag{15}$$

where integer variables n_u stand for the topological charges of the vortices and are defined on the plaquettes u. Now $\tilde{G}_{uu'}$ is proportional to the lattice Green function of the dual lattice.

As in the case of the original lattice, the calculation of $\tilde{G}$ can be made with the help of the generating function, which is quite analogous to Eq. (8):

$$\tilde{Z}\{f\}=\prod_u\left[\int_{-\infty}^{\infty}dx_u\right]\exp\left[\frac{1}{2K}\sum_{(u,u')}(x_u-x_{u'})^2+2\pi i\sum_u f_u x_u\right], \tag{16}$$

where the first summation is now over pairs of nearest neighbors on the dual lattice. Then $\tilde{G}_{uu'}$ can be expressed as

$$\tilde{G}_{uu'}=-\left[\frac{\partial}{\partial f_u}\frac{\partial}{\partial f_{u'}}\tilde{Z}\{f\}\right]_{f=0}. \tag{17}$$

The first step is to integrate out the variables defined at the elementary plaquettes. That yields

$$\tilde{Z}\{f\}\propto\tilde{V}_1\{f\}\prod_u\left[\int_{-\infty}^{\infty}dx_u\right]\exp\left[-\frac{1}{5K_1}\sum_{\langle\langle u,u'\rangle\rangle}(x_u-x_{u'})^2+2\pi i\sum_u f'_u x_u\right] \tag{18}$$

with

$$K_1=\tfrac{3}{5}K, \quad f'_u=\tfrac{1}{3}\sum_{u'}f_{u'}+f_u\ , \tag{19}$$

where the sum over u' is to be taken over all elementary plaquettes surrounding the sth order plaquette u. The form of the expression for f' corresponds to splitting each field f_u defined on an elementary plaquette into three equal parts that shift to the three neighboring plaquettes.

Thus we have obtained again the lattice that is dual to a Sierpinski gasket of a smaller order. But now we have coupling not only between nearest neighbors but also between second-nearest neighbors (see Fig. 3) which correspond to plaquettes of different size which are adjacent to the same elementary plaquette. All the couplings are equal. The exponent of the factor

$$\tilde{V}_1\{f\}=\exp\left[\sum\frac{4\pi^2K}{2}\frac{1}{3}(f_u)^2\right] \tag{20}$$

gives the first additive contribution to $\tilde{G}_{uu'}$, where the summation is to be taken over all elementary plaquettes.

Luckily at all other steps of the integration the struc-

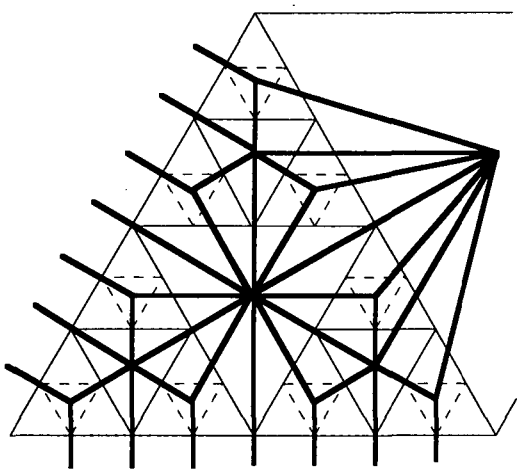

FIG. 3. Pairs of sites of the dual lattice that become coupled after the first decimation are connected by bold lines.

ture of the expression for $\tilde{Z}_s\{f\}$ will be conserved. No additional coupling will appear, and K will scale with a factor of $\frac{3}{5}$. So the scaling on the dual lattice and on the original lattice are completely consistent with each other. After summing all contributions $\tilde{G}$ can be expressed as follows:

$$\tilde{G}_{\mathbf{u}\mathbf{u}'}=4\pi^2K\left[\tfrac{1}{3}\delta_{\mathbf{u}\mathbf{u}'}+\tfrac{1}{2}\sum_{s=s_{\mathbf{u}\mathbf{u}'}}^{\infty}(\tfrac{3}{5})^{s-1}a_{\mathbf{u}}(s)a_{\mathbf{u}'}(s)\right], \tag{21}$$

where $s_{\mathbf{u}\mathbf{u}'}$ is the minimal order of a piece of fractal including both $\mathbf{u}$ and $\mathbf{u}'$. If $s=s_{\mathbf{u}\mathbf{u}'}$ then $a_{\mathbf{u}}(s)=1$ and if $s>s_{\mathbf{u}\mathbf{u}'}$ then $a_{\mathbf{u}}(s)$ is the contribution, after s transformations, of $h_{\mathbf{u}}$ to the sth order plaquette belonging to the sth order fractal containing $\mathbf{u}$. That means that $a_{\mathbf{u}}(s)$ has the form

$$a_u(s)=\sum_l(\frac{1}{3})^{N_l}, \tag{22}$$

where summation is to be taken over all paths that begin at $\mathbf{u}$, go step by step to a larger plaquette along the second-nearest neighbors (except for the first step in the case where $\mathbf{u}$ is an elementary plaquette when the paths go to a nearest neighbor) and reach the sth order plaquette which is at the center of the s-order fractal including $\mathbf{u}$. N_l is the number of steps forming the lth path. Then $\tilde{G}_{\mathbf{u}\mathbf{u}'}$ is always finite because it is evident that $a_{\mathbf{u}}(s)$ never exceeds 1. Therefore

$$\frac{1}{4\pi^2K}\tilde{G}_{\mathbf{u}\mathbf{u}'}<\tfrac{1}{3}+\tfrac{1}{2}\sum_{S=0}^{\infty}(\tfrac{3}{5})^s=\tfrac{19}{12} \tag{23}$$

for any $\mathbf{u}$ and $\mathbf{u}'$.

The same approach as in Sec. II can be used to understand the dependence of the vortex self-energy ($\propto\tilde{G}_{\mathbf{u}\mathbf{u}}$) on the plaquette size and that of the interaction energy ($\propto\tilde{G}_{\mathbf{u}\mathbf{u}'}$) on the separation distance $|\mathbf{u}-\mathbf{u}'|$. One considers two plaquettes $\mathbf{u}$ and $\mathbf{u}'$ with the order s' and s'', respectively. Then one performs the renormalization procedure $s=s_{\mathbf{u}\mathbf{u}'}$ times, obtaining the expression of Z_{vort} for the model with $K_R=(\frac{3}{5})^SK$ and distance between plaquette centers equal to $(\frac{1}{2})^S|\mathbf{u}-\mathbf{u}'|$. This shows that the interaction energy decays as

$$\tilde{G}(r)\propto(\tfrac{3}{5})^S\equiv r^{-\nu},\quad r>0, \tag{24}$$

with the same exponent $\nu=\ln(\frac{5}{3})/\ln 2$ as the correlation function of the harmonic approximation. This also means that the vortex self-energy is multiplied by a factor $\frac{3}{5}$ when the plaquette order is increased by one.

Our calculation has shown that the energy of a vortex is always finite on a Sierpinski gasket. Thus free vortices will always be present and no phase transition related to the dissociation of vortex molecules will take place (in contrast to the case of regular 2D lattice). Moreover the energy of a vortex scales with a factor $\frac{3}{5}$ with the increase of the size of the plaquette. So for any temperature for large enough plaquettes the concentration of vortices will be large in comparison with unity. So, at least starting from the scale ξ, the behavior of the correlation function will be strongly modified by vortices. In order to investigate the decay of correlation function at large scales we shall introduce another approximation, which is suitable for the limit of weak coupling.

IV. EXACTLY RENORMALIZABLE MODEL

Let us consider an XY model on a Sierpinski gasket described by the Hamiltonian

$$H=-k_BT\sum\ln\left[1+K\sum\cos(\theta_{\mathbf{r}}-\theta_{\mathbf{r}'})\right], \tag{25}$$

where the external sum is to be taken over all elementary plaquettes and the internal one over the perimeter of each such plaquette. If one develops the logarithm in powers of K, the first-order terms would give the Hamiltonian (1), while the higher-order terms will introduce also three-particle interaction on each elementary plaquette. Thus one can consider the Hamiltonian (25) as an approximation to the Hamiltonian (1) (which is exact in the limit $K\to 0$). The statistical weights $W=\exp(-H/k_BT)$ defined by (25) remain positive only for $K<K_*=\frac{2}{3}$, so it cannot be used directly for the investigation of the low-temperature properties of (1).

Hamiltonian (25) allows for the same exact renormalization as the Hamiltonian (4) of the harmonic approximation. But in contrast to the harmonic case the vortices are now also implicitly taken into account, because the phase-phase coupling in (25) is really periodic. In the case of (25) after performing the integration over first-order variables one obtains the Hamiltonian with the same structure, but with the rescaled value of coupling:

$$K_1=\frac{2+K}{4+K^3}K^2. \tag{26}$$

For $K\ll 1$ Eq. (26) reduces to $K_1\approx(\frac{1}{2})K^2$, so if one starts from $K_0\ll 1$ after s steps one obtains

$$K_s\approx 2(K_0/2)^{2^s}.$$

From Eq. (26) follows that for any $K<K_*$ the renormalized coupling is smaller than the initial one. This

means that the coupling always scales down to zero and there is no phase transition.

As for the calculation of the correlation function, the simplest thing to do would be to estimate its value for the sites on the corners of the same sth order plaquette (that is, at distance $r=2^s$). Then after performing the renormalization s times one will have them as the nearest neighbors, so the correlation function will be proportional to renormalized coupling:

$$g(r) \propto K_s \propto \exp\left[-\left|\ln\frac{2}{K_0}\right| r\right] . \tag{27}$$

That means that the correlations decay in an ordinary exponential way and that correlation radius R_c is equal to $1/\ln(2/K_0)$.

The decay of the correlations, described by Eq. (27) turned out to be more rapid than in the domain of the validity of the harmonic approximation. That can be considered as the manifestation of the finite concentration of vortices. Equation (27) will hold for the model (25) with $K \ll 1$, that is for the model (1) with $J \ll k_B T$. For $K \sim K_*$ it will give $R_c \sim 1$.

If one is interested in the low-temperature properties of models (1) or (3) one can use the harmonic approximation renormalization till K_R becomes of the order of one and then switch to the model (25) and use the fact that for it R_c will be of the order of one in the units of $\xi = K^{1/\nu}$. The correlation function will decay according to Eq. (13) for $r \ll \xi$ and according to Eq. (27) with $R_c \sim K^{1/\nu}$ for $r \gg \xi$.

V. CONCLUSION

We have studied an XY model on a Sierpinski gasket. A main difference with the case of a regular lattice is that the self-energy of a vortex is finite and the interaction energy decays as a power law of the distance. Therefore no phase transition can take place.

For any temperature the correlation function decays exponentially at large distances [$\exp(-r/R_c)$]. But in case of small temperature for distances smaller than the correlation radius ($R_c \sim (J/k_B T)^{1/\nu}$) it decays as $\exp(-r^\nu/C)$ with $C \propto K$ and $\nu = \ln(\frac{5}{3})/\ln 2 < 1$.

On the other hand in the case of a regular lattice formed by the sth order fractals (as in Ref. 5) the Berezinskii-Kosterlitz-Thouless transition should take place, but at a quite different temperature than in the periodic triangular lattice with the same lattice parameter. One should bear in mind that such complex lattice would be equivalent to the triangular lattice with the coupling constant rescaled by the factor of $(\frac{3}{5})^s$.

The approach developed in this paper can be expected to be of relevance for the description of superconducting wire networks only if the coherence length is not small in comparison with the wire width. In the opposite case the network will behave like a bulk sample without manifestation of fluctuations.

ACKNOWLEDGMENTS

This work has been supported by the Swiss National Science Foundation.

[1]For a recent review, see Coherence in Superconducting Networks, NATO advanced research workshop, Delft 1987 [Physica B **152** (1988)].

[2]J. M. Gordon, A. M. Goldman, J. Maps, D. Costello, R. Tiberio, and B. Whitehead, Phys. Rev. Lett. **56**, 2280 (1986).

[3]P. Martinoli *et al.* (private communication).

[4]S. Alexander, Phys. Rev. B **27**, 1541 (1983).

[5]S. Alexander and E. Halevi, J. Phys. (Paris) **44**, 805 (1983).

[6]V. L. Berezinskii, thesis, L. D. Landau Institute, Moscow, 1971.

[7]J. Villain, J. Phys. (Paris) **36**, 581 (1975).

[8]B. Nienhuis, J. Stat. Phys. **34**, 731 (1984).

Classical Frustrated XY Model: Continuity of the Ground-State Energy as a Function of the Frustration

A. Vallat and H. Beck

Institut de Physique, Université de Neuchâtel-Breguet 1, CH-2000 Neuchâtel, Switzerland

(Received 12 November 1991)

The uniformly frustrated classical XY model can describe Josephson-junction arrays in a transverse magnetic field. It has been suggested that the energy $E(f)$ and the $T=0$ critical current $i_c(f)$ in the ground state may be highly discontinuous functions when the frustration parameter f goes through rational and irrational values. We show here that $E(f)$ is a continuous function for a wide class of spin-spin interacting potentials including the cosine for which $E(f)$ will be strictly negative for all f. We discuss the behavior of $i_c(f)$ and we show that $i_c(f)$ has a strictly positive lower bound in the case of piecewise parabolic interacting potential.

PACS numbers: 75.10.Hk, 64.70.Rh, 74.50.+r

The classical frustrated XY model given by the Hamiltonian

$$H=\sum_{\langle rr'\rangle} V(\theta_r-\theta_{r'}-A_{rr'}), \tag{1}$$

with $V(x)=-\cos x$, has been studied rather extensively during recent years [1-4]. It describes, for example, Josephson-junction arrays or wire networks placed in a homogeneous perpendicular magnetic field [5,6]. In fact, the piecewise parabolic potential $V(x)=\frac{1}{2}(x+2\pi n)^2$, where n is an integer such that $x+2\pi n\in(-\pi,\pi]$ should be more suitable for the wire networks at very low temperatures. The variable θ_r represents the phase of the macroscopic wave function on site r and the quantity $A_{rr'}$ is proportional to the line integral of the vector potential from site r to site r'. The sum in Eq. (1) is taken over pairs of nearest neighbors, and the Josephson coupling, which would multiply the cosine, has been set equal to 1. The strength of the magnetic field is measured by the gauge-invariant quantity

$$\sum_{\square R} A_{rr'}=2\pi f, \tag{2}$$

where the notation $\sum_{\square}$ means that the sum is taken in a clockwise direction over the bonds surrounding the plaquette R of the lattice. The frustration parameter f measures the flux through a plaquette in units of the elementary flux quantum. The XY model (1) has also been studied in connection with high-temperature superconductivity [7], where it is supposed to describe the physics of an individual CuO plane (respectively, double plane) on a phenomenological level, and with the description of flux phase states in the t-J model [8].

The detailed thermodynamic behavior of the frustrated XY system for various (rational or irrational) values of f is one of the most intriguing problems of classical statistical mechanics. Let alone the different scenarios that could describe the possible phase transitions at finite temperature, for a given f, there is not even a generally applicable strategy to determine all possible ground states. For some particularly simple rational values of f, like $\frac{1}{2}$, $\frac{1}{3}$, $\frac{1}{4}$, etc., ground states have been found, in terms of either the corresponding configurations of the angle variables θ_r or a charge picture, introduced below [4]. In general, these ground states possess not only the continuous rotational symmetry of the Hamiltonian, but also some discrete degeneracy. Some unexpected wealth of ground-state configurations has recently been discovered for $f=\frac{1}{3}$ and $\frac{1}{4}$ for the triangular lattice [9]. For a rational value $f=p/q$ the periodicity of a ground-state configuration essentially depends on the denominator q. Therefore one may expect a rather "wild" variation of these configurations when f is varied through the real axis, going through rational and irrational values. Such complicated dependence on the particular value of f would make the interpretation of experimental data very difficult, since the magnetic field—and thus the frustration f—is never measured with infinite precision. However, we have to bear in mind that the details of the angular configuration of the system are usually not observed. Therefore, the essential question that arises is the following: What is the functional dependence on f of observable "macroscopic" quantities, like the ground-state energy $E(f)$, the critical current $i_c(f)$, or the helicity modulus $\gamma(f)$? Several authors have pointed out that $E(f)$ and $i_c(f)$ are indeed discontinuous functions of f, much like the ground-state configurations themselves. This would in principle be an interesting result, but, as stated above, it would pose serious problems for the interpretation of experimental data.

The main point of this Letter is to show that, for any regular lattice, the ground-state energy of Hamiltonian (1) is a continuous function of f (the demonstration is presented for the infinite square lattice and for a cosine potential). The implications of this result on i_c and γ at zero temperature will be discussed at the end.

It is useful to rewrite our Hamiltonian in "gauge-invariant" bond variables $\phi_{rr'}$:

$$H=-\sum_{\langle rr'\rangle} V(\phi_{rr'}). \tag{3}$$

In order that expressions (1) and (3) agree, the following constraints have to be imposed for each plaquette R:

$$\sum_{\square R}\phi_{rr'} = -2\pi f + 2\pi m_R . \tag{4}$$

The quantity m_R is an arbitrary integer. Each state could be represented in such a way that every $\phi_{rr'}$ is included in the interval $(-\pi,\pi]$; therefore m_R would belong to the set $\{-1,0,1,2,\}$ and represent the topological charge on that plaquette. But in this paper it will be more convenient to consider that the $\phi_{rr'}$'s are arbitrary real numbers.

We now prove (considering the cosine potential) that $E(f)$ is a uniformly continuous function when f goes through the real numbers (since the system is even in f and periodic with period 1, only the interval $0 \le f \le \frac{1}{2}$ has to be considered); i.e., $\forall \varepsilon > 0$, $\exists \delta(\varepsilon)$ such that for all real $f,\bar{f}$, one has

$$|\bar{f}-f| < \delta(\varepsilon) \Rightarrow |E(\bar{f}) - E(f)| < \varepsilon . \tag{5}$$

We start with a given frustration f. Let $\Phi_f \equiv \{\phi_{rr'}\}$ be one of the possible ground-state configurations for that value of f, with energy $E(f)$ per bond. By construction this configuration satisfies all constraints with some given set of numbers m_R. We then choose another frustration $\bar{f}$ and construct a new configuration $\bar{\Phi}_{fn} \equiv \{\bar{\phi}_{rr'}\}$. The latter will not be, in general, a ground-state configuration for the new frustration $\bar{f}$, and its energy per bond, denoted by $E_{fn}(\bar{f})$, will be higher than the corresponding ground-state energy $E(\bar{f})$. The procedure for constructing $\bar{\Phi}_{fn} \equiv \{\bar{\phi}_{rr'}\}$ is the following.

(a) Choosing a positive integer n the (infinite) square lattice is cut into vertical strips containing $2n+1$ sites on each horizontal line; see Fig. 1 (the sites r, carrying the variables θ_r, lie on the nodes of the lattice). Within each strip the vertical lines are numbered with positive and negative indices, such that the middle line is indexed zero. The horizontal distance $d_{rr'}$ of a given vertical bond rr', in units of the lattice constant, is then given by the index corresponding to the line on which the vertical bond is sitting. We call "internal bonds" and "internal plaquettes" those which do not cross or sit on one of the dashed lines separating two strips.

(b) The following transformation is applied to the internal bonds:

$$\phi_{rr'} \mapsto \bar{\phi}_{rr'} = \begin{cases} \phi_{rr'} & \text{on the horizontal bonds,} \\ \phi_{rr'} + 2\pi(f-\bar{f})d_{rr'} & \text{on the vertical bonds.} \end{cases} \tag{6}$$

By construction the constraints (4) for all internal plaquettes are still satisfied for the new configuration.

(c) For the remaining columns of horizontal bonds, i.e., those that cross a borderline between strips, we choose freely the value $\phi_{rr'}$ for one bond on each column. For the other horizontal bonds of each column the values are then fixed by requiring that the constraints be satisfied for all plaquettes lying on the borderline. This can be done in such a way that the average value of $\cos\phi_{rr'}$ over all horizontal bonds of a given frontier is positive. (If this average turned out to be negative, after the construction has been done, it suffices to add π to each $\phi_{rr'}$. This does not violate the constraints, but it changes the sign of $\cos\phi_{rr'}$ everywhere.)

We can now give an upper bound for the mean charge of the energy $-\cos\phi_{rr'}$ of the horizontal and vertical bonds attached to a given horizontal line of any strip, induced by the above construction (an example of such a set of bonds is given by bold lines in Fig. 1; the whole lattice can be paved by such comblike elements):

$$E_{fn}(\bar{f}) - E(f) \le \frac{1}{2(2n+1)} \left[\sum_{\text{vert bds}} 2\pi|\bar{f}-f||d_{rr'}| + 1 \right]. \tag{7}$$

For the change on the vertical bonds we have used $\cos(\alpha) - \cos(\alpha+X) = \int_\alpha^{\alpha+X} \sin(t)\,dt \le |X|$. And the change due to the horizontal line lying on the strip boundary is bounded by 1, according to step (c). This yields the following inequality for the difference between the two energies (per bond):

$$E_{fn}(\bar{f}) - E(f) \le \frac{1}{2(2n+1)} [n(n+1)2\pi|\bar{f}-f| + 1] . \tag{8}$$

Given now an ε with $0 < \varepsilon \le \frac{1}{2}$ we choose the width of our strips by taking

$$n(\varepsilon) \in [1/2\varepsilon - 1, 1/2\varepsilon] . \tag{9}$$

Then the right-hand side of Eq. (8) will be smaller than ε whenever the difference $|\bar{f}-f|$ is smaller than

$$\delta(\varepsilon) = 2\varepsilon^2/\pi . \tag{10}$$

Therefore $\forall \varepsilon > 0$, $\exists \delta$ such that for all real numbers $f,\bar{f}$, one has

$$|\bar{f}-f| < \delta \Rightarrow E_{fn}(\bar{f}) - E(f) < \varepsilon$$

and, since by definition of the ground-state energy $E(\bar{f})$ for the frustration $\bar{f}$ is lower than $E_{fn}(\bar{f})$, we have found $\delta(\varepsilon)$ such that

$$|\bar{f}-f| < \delta \Rightarrow E(\bar{f}) - E(f) < \varepsilon . \tag{11}$$

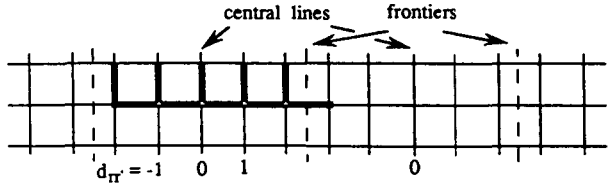

FIG. 1. The infinite lattice is cut into vertical strips. Here $n=2$. The "internal bonds" and "internal plaquettes" are those which do not cross or sit on a dashed line separating two strips. The sites r, carrying the variables θ_r, lie on the nodes of the lattice.

It is crucial to note, at this stage, that we are not allowed to put absolute value signs around the difference of energies $E(\bar{f})-E(f)$. Indeed, the state $\bar{\Phi}_{fn}$ that we have constructed may be a very "bad" approximation to any of the ground states for frustration $\bar{f}$ (since the ground-state configurations may indeed vary drastically for two values of f which are very close to each other). $E(\bar{f})$ may be much lower than $E(f)$, such that the difference $E(\bar{f})-E(f)$ is a negative number with a possibly large absolute value, lying—according to the inequality—lower than ε on the real axis.

As a last step in our proof we repeat the same procedure, starting this time from a given ground-state configuration for frustration $\bar{f}$, with energy $E(\bar{f})$ per bond. We end up with the same inequality (11) [with the same $\delta(\varepsilon)$], but with f and $\bar{f}$ reversed:

$$|\bar{f}-f|<\delta \Rightarrow E(\bar{f})-E(f)\leq\varepsilon. \tag{12}$$

Combining (11) and (12) we can now conclude that

$$|\bar{f}-f|<\delta \Rightarrow |E(\bar{f})-E(f)|\leq\varepsilon, \tag{13}$$

which indeed means that $E(f)$ is a uniformly continuous function of its argument. Moreover the two known values, $E(0)=-1$ and $E(\frac{1}{2})=-1/\sqrt{2}$, together with the symmetry and the periodicity in f and the fact that

$$\delta(\varepsilon)=2\varepsilon^2/\pi, \tag{14}$$

allow the conclusion that $E(f)$ is strictly negative for all f for the cosine potential.

Our explicit demonstration has been presented for a square lattice and for a cosine interaction potential. The same steps can be applied to any regular lattice and to other periodic interaction potentials whose derivative is bounded.

We conclude with some remarks concerning the critical current and the helicity modulus. Following Teitel and Jayaprakash [2] the critical current of the array is usually defined by

$$i_c(f)=\max_{\delta}\left[(i_{c0}/N)\sum_{\text{vert bds}}\sin[\phi_{rr'}(\delta)+\delta]\right], \tag{15}$$

where i_{c0} is the single junction critical current and N is the number of sites. $\Phi_f(\delta=0)\equiv\{\phi_{rr'}(\delta=0)\}$ is one of the ground-state configurations and $\Phi_f(\delta)$ evolves continuously from $\delta=0$ as a local minimum of the energy. The quantity δ corresponds to a "twist" of $n\delta$ ($n^2=N$) applied to the phases θ_r on the two opposite vertical boundaries. First we approximate i_c neglecting the δ dependence of the $\phi_{rr'}$'s. So we define i_c' as in (15), but with $\Phi_f(\delta)=\{\phi_{rr'}(\delta=0)\}\equiv\{\phi_{\bar{r}\bar{r}'}\}$. Since $\sin x=\cos(x-\pi/2)$ we have

$$i_c'(f)=\max_{\delta}\left[(i_{c0}/N)\sum_{\text{vert bds}}\cos(\phi_{rr'}+\delta-\pi/2)\right]. \tag{16}$$

The sum on the right-hand side reaches its maximum for $\delta=\pi/2$, where it equals N times the absolute value of the mean energy per horizontal bond in the ground state. If, in the ground state, the energy on the horizontal and of the vertical bonds are equivalent, we obtain

$$i_c'(f)=i_{c0}|E(f)|. \tag{17}$$

If for some ground state the horizontal and vertical bond energies differ, we should replace (16) by an average over the different ground states (otherwise we could not speak about the critical current of the system but of one particular ground state). If there is such a ground state, there is another one, for which horizontal and vertical bond energies are interchanged. For such a couple of ground states Eq. (17) is again valid.

Two remarks are in order. First, our result (17) gives and upper bound to i_c. The estimate

$$i_c(p/q)\leq i_{c0}|E(f)|\pi/q \tag{18}$$

of Ref. [2] would give a better result. However, the crucial argument given in Ref. [12] of Ref. [2] seems to us not to be correct. In particular, for very small frustration $f=1/q$ with large q, a value of δ equal to π/q would be too small to destabilize the topological configuration.

Second, our approximation considers a fixed configuration of the $\phi_{rr'}$'s (kept equal to their ground-state value). However, given the external twist, the phase differences will adapt and the true physical maximum current may be lower than the one given by (17). This leaves open the question of whether for certain values of the frustration this "relaxed" critical current could indeed be zero. In order to clarify this problem, it is very instructive to replace the cosine interaction potential by a piecewise parabolic potential. In such a case, the phase differences remain all in local equilibrium, i.e., the sum over the four $\phi_{rr'}$ [i.e., the derivative of the piecewise parabola $V'(x)=x$ as long as $|x|\neq\pi$] going out of any site will be zero while δ does not exceed $\pi/4$. Indeed it can be easily verified that $|\phi_{rr'}|$ is smaller than $3\pi/4$ at the ground state (note that $|\phi_{rr'}|>3\pi/4$ would imply that the energy can be lowered by a rotation of $\pm\pi/2$ or $\pm\pi$ of the spin angle θ_r or $\theta_{r'}$). This gives the following lower bound for the $T=0$ critical current [the sine in Eq. (15) is replaced by the derivative of the piecewise parabola]:

$$i_c\geq i_{c0}\pi/4. \tag{19}$$

Thus, our estimation (17) of the $T=0$ critical current neglects a relaxation effect the relevance of which depends on the form of the interaction potential and is irrelevant for the piecewise parabola.

The helicity modulus γ, expressing the rigidity of the system with respect to the applied "twist" between two opposite boundaries, is given by Ref. [3]:

$$\gamma=\frac{1}{N}\left[\left\langle\sum_{\langle rr'\rangle}x_{rr'}^2V''(\phi_{rr'})\right\rangle-\frac{1}{T}\left\langle\left[\sum_{\langle rr'\rangle}x_{rr'}V'(\phi_{rr'})\right]^2\right\rangle\right], \tag{20}$$

where $x_{rr'}=x_{r'}-x_r$ and x_r is the horizontal component of the position of the site r. At $T=0$, for the cosine potential, the first term is minus half the ground-state energy (since the thermodynamic average on the horizontal and the vertical bonds are again equivalent). This contribution to γ is therefore a continuous function, which is positive for all f. It seems much more difficult to estimate the value of the second term in the limit as T goes to zero in the case of the cosine potential. Numerical simulations for several values of f indicate that it is strictly smaller than the first term, but more systematic investigations are necessary in order to make a definite statement about the behavior of γ as a function of f at $T=0$. Again the case of the piecewise parabolic potential is useful to consider because there it is possible to show that the second term vanishes when T goes to 0. Thus, for a lattice of arbitrary but finite size, $\gamma=1$ for any f.

In summary, we have shown that for the case of a regular lattice the ground-state energy per bond of the uniformly frustrated XY model is a continuous, strictly negative function of the frustration parameter f. For a cosine interaction potential, this implies that the $T=0$ critical current, evaluated for a fixed ground-state configuration (i.e., evaluated by neglecting possible relaxation effects) is also continuous in f and is, particularly, nonzero for all f. Furthermore, the relevance of this relaxation effect depends on the considered interaction potential. In particular, the relaxation effect is irrelevant for a piecewise parabolic potential.

We are grateful to M. Kosterlitz, S. Shenoy, S. Korshunov, J. Villain, and Ph. Choquard for interesting discussions concerning our proof. This work was supported by the Swiss National Science Foundation.

[1] S. Teitel and C. Jayaprakash, Phys. Rev. B **27**, 598 (1983); W. Y. Shih and D. Stroud, Phys. Rev. B **28**, 6575 (1983); **30**, 6774 (1984); M. Y. Choi and S. Doniach, Phys. Rev. B **31**, 4516 (1985); S. E. Korshunov and G. V. Uimin, J. Stat. Phys. **43**, 1 (1986); S. E. Korshunov, J. Stat. Phys. **43**, 17 (1986); M. Y. Choi and D. Stroud, Phys. Rev. B **35**, 7109 (1987); S. Teitel, Physica (Amsterdam) **152B**, 30 (1988).

[2] S. Teitel and C. Jayaprakash, Phys. Rev. Lett. **51**, 1999 (1983).

[3] W. Y. Shih, C. Ebner, and D. Stroud, Phys. Rev. B **30**, 134 (1984).

[4] T. C. Halsey, Phys. Rev. B **31**, 5728 (1985); J. Phys. C **18**, 2437 (1985).

[5] For a review see *Coherence in Superconducting Networks,* NATO Advanced Research Workshop, Delft, 1987 [Physica (Amsterdam) **152B** (1988)].

[6] P. Martinoli, P. Lerch, C. Leemann, and H. Beck, Jpn. J. Appl. Phys. **26**, 1999 (1987); R. Theron, J. B. Simond, J. L. Gavilano, Ch. Leemann, and P. Martinoli, Physica (Amsterdam) **165B**, 1641 (1990).

[7] For example, M. Rasolt, T. Edis, and Z. Tesanovic, Phys. Rev. Lett. **66**, 2927 (1991).

[8] For example, P. Lederer, D. Poilblanc, and T. M. Rice, Phys. Rev. Lett. **63**, 1519 (1989).

[9] A. Vallat, S. E. Korshunov, and H. Beck (unpublished).

PHYSICAL REVIEW B VOLUME 50, NUMBER 6 1 AUGUST 1994-II

Coulomb-gas representation of the two-dimensional XY model on a torus

A. Vallat
Department of Physics, Brown University, Providence, Rhode Island 02912

H. Beck
Institut de Physique, Université de Neuchâtel, Breguet 1, CH-2000 Neuchâtel, Switzerland
(Received 27 January 1994)

Superconducting networks and superfluid films in two dimensions are often described by a theoretical model in which the unique microscopic variables are phases. Among these models the XY model with Villain's interaction potential can be mapped exactly onto a lattice Coulomb gas. This is well known, but several questions still have no clear answers: First, what is the meaning of the charge of the Coulomb gas in terms of the original variables of the XY model? Second, how can the helicity modulus be expressed exactly in the Coulomb-gas representation on a finite torus? In this paper we answer these questions. The mapping onto a lattice Coulomb gas is done in a way that differs from the usual one. This mapping is applied to a phase model whose partition function has an identical mathematical structure as the one of the XY model with Villain's interaction. For this phase model, contrary to the XY model, the charges of the Coulomb gas describe indeed exactly the topological charges as we can define them in terms of the phase variables. However, this Coulomb gas contains an additional polarization energy and two additional fictitious variables accounting for the specific topological character of the torus. The helicity modulus is exactly the inverse of a dielectric constant which can be defined as the linear response to an external uniform electric field, even on a torus. The meaning of the Coulomb-gas representation is also discussed in terms of the original variables of the XY model.

I. INTRODUCTION

The two-dimensional (2D) XY model can describe various superconducting networks,[1] in particular Josephson junction arrays (e.g., Ref. 2) which correspond to a cosine interaction potential between the phase variables on neighboring sites. It seems also to be relevant for the theoretical understanding of superconductors with high critical temperature (e.g., Refs. 3 and 4).

In 1973 Kosterlitz and Thouless[5] decoupled the XY model into two subsystems, approximating the lattice by a continuum. Each state was given by a topological configuration (configuration of vortices) and small amplitude fluctuations around the vortices. The fluctuation part describes the linear spin waves of the system, and the topological part was mapped onto a Coulomb gas.

In 1975, Villain[6] proposed an approximation for the cosine interaction potential that has been used rather often since then. José, Kadanoff, Kirkpatrick, and Nelson[7] based an exact decoupling into a spin-wave part and a Coulomb-gas part on this approximation. However, in this case, the charges of the Coulomb gas do not correspond exactly to the topological charges as they are defined in the original variables. Moreover, the spin waves do not correspond to the fluctuations around a local minimum of the energy.

The crucial quantity for describing the behavior of the XY model system as a function of the temperature is the helicity modulus Γ, whereas for the Coulomb gas the relevant quantity is the inverse dielectric constant $1/\varepsilon$. The helicity modulus was introduced in 1973 by Fisher, Barber, and Jasnow[8] in order to define the superfluid density ρ_s of the superfluid helium film. The theoretical link between ρ_s and the dielectric constant $1/\varepsilon$ of a Coulomb gas has been studied, in a continuum version and in different ways, principally by Nelson and Kosterlitz,[9] Myerson,[10] and Minnhagen and Warren.[11] The definition of Γ has been extended to the XY model by Ohta and Jasnow[12] who consider the cosine potential at low temperature. They also gave a link between Γ and $1/\varepsilon$ at higher temperature using Villain's interaction instead of the cosine. Later, Shih, Ebner, and Stroud[13] expressed the helicity modulus of the XY model in terms of thermodynamical averages. Their expression has been extensively used in Monte Carlo simulations of the XY model with periodic boundary conditions imposed on the planar spin variables.

Several aspects are still unclear. First, the integers m_R introduced by José *et al.*[7] are arbitrary numbers (even if the angles of the spins are restricted to the interval $(-\pi,\pi]$). They are called "quantum number for a vortex excitation."[7] However, the topological charge q_R of a vortex as we can define it in terms of the original variables takes only values in the set $\{-1,0,1\}$ for the square lattice. Even if in practice the values of the m_R's are often restricted to this set, m_R and q_R do not have exactly the same meaning. This fact has been pointed out by Savit,[14] but the meaning of the charge of the Coulomb gas has not been given in terms of the original variables.

Second, the influence of different boundary conditions has not been carefully studied. Indeed, the periodic boundary conditions in terms of the original variables

0163-1829/94/50(6)/4015(15)/$06.00

have not been taken into account in the calculations of Ref. 7. However, the calculation of the helicity modulus as expressed in terms of thermodynamical averages depends on the boundary conditions, and it is crucial to calculate it with boundary conditions in the original variables. Fisher *et al.*[4] have considered an additional term in the Coulomb-gas Hamiltonian taking into account the periodic boundary conditions. Their Hamiltonian represents correctly the XY model (with Villain's interaction) for fixed boundary conditions, but their Coulomb gas misses some variables in the case of periodic ones.

Third, a well known result in statistical physics allows one to express the dielectric constant in terms of the quadratic average of the polarization. As the helicity modulus of the XY model can be defined on a torus, what is the polarization of a configuration of the associated Coulomb gas in such a manifold? Moreover, if the twist corresponds to a uniform electric field, how can we explain that the helicity modulus can be defined as a linear response to a twist since we know that the linear response of a Coulomb gas with periodic boundary conditions to a uniform electric field is not defined ($\varepsilon \to \infty$)?

The problem of the boundary conditions of the 2D Coulomb gas is well known and has been studied by Choquard, Piller, and Rentsch,[15] who found a dependence of the dielectric susceptibility on the boundary conditions even in the thermodynamic limit.

Thus, the aim of this paper is to clarify the Coulomb-gas representation of 2D XY models whose unique microscopic variables are phases. For this purpose, in Sec. II A we consider a particular version of the XY model where the planar spins are defined on a square wire network, not only at the nodes but at each point along the wires linking nearest neighbor nodes. We will call this version the "wire model" and we will keep the denomination XY model for that involving spins only at the nodes of a lattice. Experimentally, the wire model describes a superconducting wire network in the case where only the phase of the macroscopic wave function (in a Ginzburg-Landau theory) is relevant. It would also correspond to a superfluid film in a periodical porous medium as studied by Gallet and Williams.[16] We will show that the partition function of the wire model is mathematically identical to the one of the XY model with Villain's interaction potential. Then we map the wire model onto a Coulomb gas on a torus but, instead of following the way of Ref. 7, we shall use the same approach as Kosterlitz and Thouless,[5] but for the discrete case and with periodic boundary conditions. We shall see that in this model the charges of the Coulomb gas represent indeed the topological charges as we can define them in the original variables. We find that the Coulomb gas involves an additional polarization energy and two additional fictitious variables accounting for the periodic boundary conditions. In Sec. II B we turn to the XY model. We define a useful bond variable and the topological charge for the generalized XY model. Here, a generalized XY model is one in which an interaction potential different from the cosine is used. Then we compare it with the wire model, considering first Villain's interaction and second the piecewise parabolic potential. The interest of the second one lies in the fact that it is Villain's interaction in the limit of low temperatures and it permits one to split the Hamiltonian exactly into a topological part and a spin-wave part. In Sec. II C we generalize the results briefly to the frustrated case. (Experimentally the frustration represents a transverse external magnetic field applied to a superconducting network.[2]) The results of this generalization will be used in the following Secs. III and IV.

In Sec. III we give the meaning of the charge of the Coulomb gas associated with the XY model in terms of the original variables. For this purpose, we consider the second order variation of the free energy with respect to frustration terms around two given plaquettes. The derivation is performed in two different ways in Sec. III A in the original one and the Coulomb-gas representation, respectively. In Sec. III B, we consider the two different interaction potentials mentioned above and the usual cosine interaction corresponding experimentally to Josephson junction arrays. The calculations of Sec. III A will allow for an interpretation of the charge of the associated Coulomb gas in terms of the topological charge as it can be defined in the original variables.

In Sec. IV we first recall the notion of helicity modulus Γ. In Sec. IV A, for the wire model on a torus we transform Γ into the inverse dielectric constant $1/\varepsilon$ of a Coulomb gas whose charges represent exactly the topological charges. We will see that Γ can indeed be represented by the second order variation of the free energy of the associated Coulomb gas with respect to a uniform external electric field. In Sec. IV B we turn again to the XY model and compare Γ in the two different representations.

This work establishes in an exact way the formal analogy between the XY model and the Coulomb gas on a 2D torus.

II. MAPPING ONTO TWO-DIMENSIONAL COULOMB GAS

In Sec. II A we begin to define the wire model. Then we map this model onto a lattice Coulomb gas. In Sec. II B we turn to the XY model. We generalize it in the sense that we consider other interaction potentials than the cosine. We shall discuss how to apply the results of Sec. II A. In particular, we shall explain why we do not find the same result as in Ref. 7. In Sec. II C we briefly generalize to the frustrated case.

A. The wire model

In this model, a planar spin $\vec{S}_l$ determined by a phase $\theta_l \in (-\pi, \pi]$ is associated to each point indexed by l of a square wire network (cf. Fig. 1). More precisely, a state of the system is described by a continuous and differentiable function $\vec{S}_l$, defined on a regular network of horizontal and vertical straight lines. L will stand for the linear size and $N \equiv L^2$ for the number of nodes. For simplicity, the lattice constant is put equal to 1. The Hamiltonian of the system is

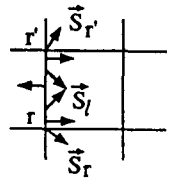

FIG. 1. In the wire model a state is described by a continuous function $\vec{S}_l$ defined on the sites (r and r') and on each point along the bonds linking them.

$$H = \frac{J}{2}\int dl \left(\frac{\partial \vec{S}_l}{\partial l}\right)^2, \tag{1}$$

where J is the coupling constant.

For the description of a wire superconducting network, the phase variation is proportional and opposite to the supercurrent. However, it has to be noted that, for such description, Hamiltonian (1) should be completed by a term accounting for a charge energy related to the divergence of the supercurrent. But every computational step in this paper could be performed with such a term.

Let us consider an oriented bond rr', linking a node r of the lattice to a nearest neighbor r' and parametrized by $l \in [0,1]$. Then let us define the bond quantity $\phi_{rr'}$ as the phase variation from r' to its nearest neighbor r:

$$\phi_{rr'} = -\int_{r}^{r'} dl \left(\vec{S}_l \times \frac{\partial \vec{S}_l}{\partial l}\right)\hat{z}, \tag{2}$$

where $\hat{z}$ is a unit vector perpendicular to the plane of the system. Thus $J\phi_{rr'}$ represents the supercurrent from r to r'. We can also define integer bond variables $p_{rr'}$ such that

$$\phi_{rr'} = \theta_r - \theta_{r'} + 2\pi p_{rr'}, \tag{3}$$

where θ_r and $\theta_{r'}$ correspond to the spin angles on the nodes r and r' and belong to the interval $(-\pi,\pi]$. In fact $\vec{S}=(\cos\theta,\sin\theta)$ and $(\vec{S}_l \times \partial\vec{S}_l/\partial l)\hat{z}=\partial\theta_l/\partial l$ except where θ_l runs across the border of the interval.

The phase on this bond can also be expressed as a continuous scalar function $\vartheta_l \in (-\infty,\infty)$ (equal to $\theta_l + 2\pi p_l$ where the integers p_l ensure that ϑ_l is continuous) and can be written as follows:

$$\vartheta_l = \theta_{l=0} - l\phi_{rr'} + \zeta_l. \tag{4}$$

The second term on the right hand side represents the variation of ϑ_l along l that minimizes the energy for a given $\phi_{rr'}$ or for given θ_r, $\theta_{r'}$, and $p_{rr'}$. The quantity ζ_l is the fluctuation around this configuration leaving unchanged the given site and bond variables. It is a continuous and differentiable function in the interval $[0,1]$, such that $\zeta_0 = \zeta_1 = 0$.

The calculation of the energy $H_{rr'}$ for the bond rr' gives

$$H_{rr'} = \int_0^1 dl \frac{J}{2}\left(\frac{\partial\zeta_l}{\partial l}\right)^2 + \frac{J}{2}(\phi_{rr'})^2. \tag{5}$$

The contribution of ζ_l to the partition function of the system is trivial (identical for each bond and independent of the site and bond integer variables). In the following, we shall no longer consider it.

It has to be noted that the equality $\vec{S}=(\cos\theta,\sin\theta)$ does not permit one to replace $\vec{S}$ by θ in Hamiltonian (1) because of the discontinuity occuring when θ runs across the border of the interval. Nor can we put $\vec{S}=(\cos\vartheta,\sin\vartheta)$, because that would impose $\vec{S}$ being a gradient of a continuous scalar function and, therefore, would not permit a nonzero winding number of the phase on a closed contour on the lattice:

$$\oint dl \frac{\partial\vartheta_l}{\partial l} = 0\,.$$

Indeed ϑ cannot, in general, be defined continuously on a closed loop. We can express $\vec{S}$ by ϑ only on an open path on our lattice.

Since we can neglect the internal fluctuations in the bonds, a state of the system can be described either by the variables $\theta_r \in (-\pi,\pi]$ and $p_{rr'} \in Z$ or by the variables $\phi_{rr'} \in (-\infty,\infty)$ [definition (3)] but, in this last case, two types of constraints have to be imposed on these bond variables. The first of them is, for each plaquette R,

$$\sum_{\square R} \phi_{rr'} = 2\pi q_R, \tag{6}$$

where the notation $\sum_{\square R}$ means that the sum is taken in the clockwise direction over the bonds surrounding the plaquette R on the lattice. The quantity q_R is an integer representing the topological charge on that plaquette. In terms of the first kind of variables, q_R is the winding number of the phase around the plaquette R and is given by $q_R = \sum_{\square R} p_{rr'}$. The definition of q_R yields also the following property:

$$2\pi \sum_{R\in D} q_R = \sum_{\partial D} \phi_{rr'}; \forall D, \tag{7}$$

where the sum on the left hand side is taken over the plaquettes inside any domain D on the lattice and the one on the right hand side over the bonds of its boundary ∂D in the clockwise direction.

The second type of constraint arises from the periodic boundary conditions imposed on the θ_r variables. To simplify their expressions we introduce the vector field $\vec{\phi}_r \equiv (\phi_{xr},\phi_{yr})$ representing the two $\phi_{rr'}$ variables associated to the bonds rr' pointing, respectively, in the positive horizontal and vertical directions from the site r. We can write them as

$$\sum_{r\in l_{xa}} \phi_{xr} = -2\pi q_{xa}\,, \quad \sum_{r\in l_{ya}} \phi_{yr} = -2\pi q_{ya}\,, \tag{8}$$

where q_{xa} and q_{ya} are integers and the two sums are taken over the sites of an arbitrary horizontal line ($r \in l_{xa}$) and a vertical line ($r \in l_{ya}$), respectively. The integer q_{xa} is the winding number (defined in the positive orientation) of the phase along the arbitrary chosen horizontal line. It is equal to the sum of the $p_{rr'}$'s over that line (keeping

r on the right hand side of r'). It has to be noted that the constraints imposed only on one horizontal and one vertical line are sufficient to satisfy the periodic boundary conditions on the θ_r's on all other lines. Indeed, from property (7), the sum of the ϕ_{xr}'s along another line l_{xj} is equal to $-2\pi q_{xa} + \sum_{R\in D} q_R$, where D is the domain bounded by the two lines, considering the line l_{xa} as the lower boundary of the domain D.

By definition, to each state $\{\theta_r, p_{rr'}\}$ corresponds one state $\{\phi_{rr'}\}$ (the latter notation implying that all the constraints are satisfied). But this mapping is not one to one because we have to know θ_r at one site to calculate the other θ_r's and the $p_{rr'}$ is starting from a state given by $\{\phi_{rr'}\}$. Therefore, there is a one-to-one correspondence between each set $\{\phi_{rr'}\}$ and an equivalent class of sets $\{\theta_r, p_{rr'}\}$, two of them being equivalent if they differ only by the same angle at each node. Then the partition function can be written either as

$$Z = \sum_{\{p_{rr'}\}} \int_{-\pi}^{\pi} [d\theta] \exp\left(-\beta \frac{J}{2} \sum_{\langle rr'\rangle} (\theta_r - \theta_{r'} + 2\pi p_{rr'})^2\right) \tag{9}$$

or as

$$Z = \sum_{\{q_R, q_{\alpha a}\}} \int_{-\infty}^{\infty} [d\phi_{rr'}] \prod_R \delta\left(2\pi q_R - \sum_{\square R} \phi_{rr'}\right) \times \prod_\alpha \delta\left(2\pi q_{\alpha a} + \sum_{r\in l_{\alpha a}} \phi_{\alpha r}\right) \times \exp\left(-\beta \frac{J}{2} \sum_{\langle rr'\rangle} \phi_{rr'}^2\right), \tag{10}$$

where the two products take into account the constraints (6) and (8) and the first sum is taken over all neutral topological configurations $\{q_R\}$. Indeed, the periodical boundary conditions in the $\phi_{rr'}$'s along with the property (7) imply the neutrality property of the topological configuration $\{q_R\}$:

$$\sum_R q_R = 0. \tag{11}$$

The $\phi_{rr'}$'s represent gauge invariant phase differences. For the superfluid films, the vector field $\vec{\phi}_r \equiv (\phi_{xr}, \phi_{yr})$ stands for the superfluid flow (see, for example, Refs. 11 and 16. It has to be noted that our boundary conditions restrict the gauge invariance as we shall see in Sec. II C. In order to map the wire model onto a lattice Coulomb gas, the partition function (10) in the bond variables $\phi_{rr'}$ will be used.

Let us fix a neutral topological configuration $\{q_R, q_{\alpha a}\}$. The variables $\phi_{rr'}$ can be expressed by their deviation $\varphi_r - \varphi_{r'}$ from the minimum energy configuration $\{\phi^0_{rr'}\}$ (because of the positive quadratic form of the Hamiltonian, the latter quantity exists and is unique):

$$\phi_{rr'} = \phi^0_{rr'} + \varphi_r - \varphi_{r'}. \tag{12}$$

So there is a one-to-one correspondence between equilibrium states $\{\phi^0_{rr'}\}$ and topological configurations $\{q_R, q_{\alpha a}\}$ satisfying the neutrality property. Moreover, for a given set $\{q_R, q_{\alpha a}\}$, we have a one-to-one correspondence between each state $\{\phi_{rr'}\}$ (satisfying the q_R's and the $q_{\alpha a}$'s) and an equivalent class of sets $\{\varphi_r\}$ (two of them being in the same class if they differ by the same quantity at each node).

The Hamiltonian of the system becomes

$$H = \frac{J}{2} \sum_{\langle rr'\rangle} (\phi^0_{rr'} + \varphi_r - \varphi_{r'})^2. \tag{13}$$

Since the set $\{\phi^0_{rr'}\}$ represents an equilibrium state, we have at each node r

$$\sum_{+r} \phi^0_{rr'} = 0, \tag{14}$$

where the notation $+r$ means that we sum over the four bonds linking r to its nearest neighbors. This condition corresponds to $\partial H/\partial\theta_r = 0$. Therefore, the sum of the cross terms in $\phi^0_{rr'}\varphi_r$ in Hamiltonian (13) vanishes and we have

$$H = \frac{J}{2} \sum_{\langle rr'\rangle} (\varphi_r - \varphi_{r'})^2 + \frac{J}{2} \sum_{\langle rr'\rangle} (\phi^0_{rr'})^2. \tag{15}$$

The system is decoupled into two subsystems. The first one represents the fluctuations around a topological configuration and has the form of a spin-wave Hamiltonian. The second one is the Hamiltonian $H_{\rm ch}$ depending only on the topological charges:

$$H_{\rm ch} = \frac{J}{2} \sum_{\langle rr'\rangle} (\phi^0_{rr'})^2. \tag{16}$$

We now want to express (16) explicitly in terms of q_R and $q_{\alpha a}$.

First of all we need to show the following property for any equilibrium state $\{\phi^0_{rr'}\}$:

$$\sum_{r\in l_{xj}} \phi^0_{yr} = \frac{\sigma_y}{L}, \tag{17}$$

where the sum is taken over the sites of any horizontal line l_{xj} [do not confuse Eq. (17) with Eq. (8), cf. Fig. 2] and $\sigma_y \equiv \sum_r \phi^0_{yr}$. Indeed, summing the left hand side of Eq. (14) over the sites r on the line l_{xj} gives

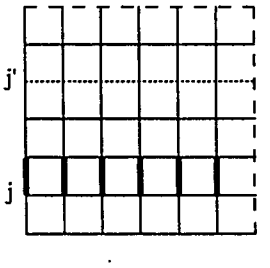

FIG. 2. The bonds marked in the dotted line correspond to those that are considered in Eq. (8) with l_{xa}=$l_{xj'}$. Those in the bold lines correspond to Eq. (17).

$$\sum_{r\in l_{xj}} \phi^0_{yr} - \sum_{r\in l_{xj-1}} \phi^0_{yr} = 0.$$

So the sum of Eq. (17) is the same for each line l_{xj}.

Then we can turn to the dual variables ψ_R defined on the plaquettes of the torus, with periodic boundary conditions, such that

$$\phi^0_{xr} = \psi_{R-\hat{y}} - \psi_R + \frac{\sigma_x}{L^2},$$
$$\phi^0_{yr} = \psi_R - \psi_{R-\hat{x}} + \frac{\sigma_y}{L^2}, \tag{18}$$

where R represents the upper right plaquette of the site r. Thus we can calculate all the ψ_R's (corresponding to any equilibrium state $\{\phi^0_{rr'}\}$) using definition (18) and choosing an arbitrary value ψ_R for one plaquette R. When we represent a state by its ψ_R's the equilibrium conditions (14) are automatically satisfied. Note that the introduction of σ_x and σ_y is necessary, otherwise the sum of the $\phi_{\alpha r}$'s over the whole lattice could only be equal to zero for any set $\{\psi_R\}$ satisfying the periodic boundary conditions.

The Hamiltonian $H_{\rm ch}$ becomes

$$H_{\rm ch} = H_{\rm ch1} + H_{\rm ch2} \tag{19}$$

with

$$H_{\rm ch1} = \frac{J}{2} \sum_{\langle RR'\rangle} (\psi_R - \psi_{R'})^2 \tag{20}$$

and

$$H_{\rm ch2} = \frac{J}{2L^2}(\sigma_x^2 + \sigma_y^2). \tag{21}$$

The sum of the cross terms $\sigma_\alpha(\psi_R - \psi_{R'})$ vanishes because of the periodic boundary conditions in the ψ_R's. Now we want to express the two terms in (20) and (21) explicitly by the topological charges. We begin with $H_{\rm ch1}$ which can be written as

$$H_{\rm ch1} = \frac{J}{2} \sum_{RR'} \psi_R M_{RR'} \psi_{R'}, \tag{22}$$

where

$$M_{RR'} = \begin{cases} 4 & \text{if } R = R', \\ -1 & \text{if } R \text{ and } R' \text{ are nearest neighbors,} \\ 0 & \text{elsewhere.} \end{cases}$$

Note that the matrix M represents the discrete Laplacian in two dimensions (with opposite sign). In the following ψ stands for the vector representing $\{\psi_R\}$ and q for $\{q_R\}$. We remark that

$$M\psi = 2\pi q, \tag{23}$$

$$\psi^t M = 2\pi q^t. \tag{24}$$

Replacing M by $MM^{-1}M$,

$$H_{\rm ch1} = 2\pi^2 J q^t M^{-1} q. \tag{25}$$

In order to link this calculation to the usual procedure in a continuum, let us consider the vector field $\vec{\phi}_r \equiv (\phi_{xr}, \phi_{yr})$ in a lattice with free boundary conditions. So the condition (14) reads $\vec{\nabla}\cdot\vec{\phi}_r = 0$. Therefore there exists a scalar field ψ_R such that $\vec{\phi}_r = \hat{z} \times \vec{\nabla}\psi_R$. Then writing the identity $\hat{z}\vec{\nabla}^2\psi_R = \vec{\nabla} \times (\hat{z} \times \vec{\nabla}\psi_R)$ and considering, in agreement with our definition of the q_R's, that $\vec{\nabla} \times \vec{\phi}_r = -\hat{z}2\pi q_R$, we obtain expression (23). Note that for periodic boundary conditions, we should also introduce quantities equivalent to σ_x and σ_y as in Eq. (18).

We shall call G the inverse matrix M^{-1}. G stands for the discrete Green function of the dual lattice. But M^{-1} does not exist because the normalized eigenvector $V_0 \equiv \{V_{0R}\}$ with $V_{0R} = 1/\sqrt{N}, \forall R$ has a zero eigenvalue [note that such an eigenvector is unique regarding (20)]. In order to solve this problem, we replace M by $M \equiv M_c - cP$ in (22), where P is the projector on V_0 ($P = V_0 V_0^t$) and c is any nonzero number. Then M_c is regular:

$$H_{\rm ch1} = 2\pi^2 J \psi^t M_c M_c^{-1} M_c \psi - \psi^t c P \psi. \tag{26}$$

Instead of Eq. (23), we have $M_c\psi = 2\pi q + cP\psi$ and $\psi^t M_c = 2\pi q^t + cP\psi^t$. Thus

$$H_{\rm ch1} = 2\pi^2 J q^t M_c^{-1} q + \pi J c P \psi^t M_c^{-1} q + \pi J q^t M_c^{-1} c P \psi + c P \psi^t M_c^{-1} c P \psi - \psi^t c P \psi. \tag{27}$$

The cross terms in ψ and q are equal to zero because the eigenvector $cP\psi$ is composed of equal components and m satisfies the neutrality property (11), and the two last terms are equal with opposite signs. Expression (27) becomes

$$H_{\rm ch1} = 2\pi^2 J q^t G_c q, \tag{28}$$

where $G_c = M_c^{-1}$ for any nonzero c. We can diagonalize the (symmetrical) matrix G_c by developing the vector ψ in plane waves. The normalized eigenvectors of M_c are identical to those of M and their corresponding eigenvalue is the same except for $\mathbf{k}=0$, for which it becomes c. For $\mathbf{k} \neq 0$, the normalized eigenvectors and the eigenvalues are

$$V_{\mathbf{k}} = \left\{ \frac{1}{\sqrt{N}} e^{-i\mathbf{k}\cdot\mathbf{R}} \right\}, \tag{29}$$

$$\lambda_{\mathbf{k}} = 4 - 2\cos k_x - 2\cos k_y, \tag{30}$$

where $\mathbf{k} \equiv (k_x, k_y)$ is a reciprocal vector of the first Brillouin zone. Then we have

$$G_{cRR'} = c + \frac{1}{N} \sum_{\mathbf{k}\neq 0} e^{i\mathbf{k}\cdot(\mathbf{R}-\mathbf{R}')} \frac{1}{\lambda_{\mathbf{k}}}. \tag{31}$$

We can choose the value of c (that we call c_0) in order to let vanish the diagonal matrix element G_{cRR}:

$$c_0 \equiv -\frac{1}{N} \sum_{\mathbf{k}\neq 0} \frac{1}{\lambda_{\mathbf{k}}}. \tag{32}$$

Let us call G' the matrix associated with c_0:

$$G'_{RR'} = \frac{1}{N}\sum_{\mathbf{k}\neq 0}(e^{i\mathbf{k}\cdot(\mathbf{R}-\mathbf{R}')} - 1)\frac{1}{\lambda_{\mathbf{k}}}. \quad (33)$$

Hamiltonian H_{ch1} alone corresponds to the charge Hamiltonian given by José *et al.*[7] for the XY model with Villain's interaction, but who found it in a different way. Their statement will be discussed in Sec. IIB. In the limit of large systems, $G'_{RR'}$ can be well approximated by a logarithmic function for any couple (R, R') with $R \neq R'$ (exact in the limit of large distances $|\mathbf{R}-\mathbf{R}'|$):

$$G'_{RR'}(L\to\infty) \approx G''(\mathbf{R}-\mathbf{R}')$$

$$\equiv -\frac{1}{2\pi}(\ln|\mathbf{R}-\mathbf{R}'| + \tfrac{1}{2}\ln 8 + \gamma), \quad (34)$$

γ being Euler's constant. This approximation [with $G''(\mathbf{0}) \equiv 0$] can be used to estimate $G'_{RR'}(L)$ for finite L. For this purpose we consider an L-periodic neutral configuration of the infinite system. The energy H_{ch1} for an $L \times L$ cell becomes

$$H_{ch1} \approx 2\pi^2 J \sum_{n_x n_y}\sum_{RR'} m_R[G''(\mathbf{R}-\mathbf{R}'+L\mathbf{n}) + c(\mathbf{n})]m_{R'}, \quad (35)$$

where R and R' run over the plaquettes of an $L \times L$ cell and $(n_x, n_y)=\mathbf{n}$ over all integer pairs. Since the configuration is neutral any function $c(\mathbf{n})$ can be added without changing the right hand side of Eq. (35). Thus we chose $c(\mathbf{n})=-G''(L\mathbf{n})$ and find the convergent estimation

$$G'_{RR'}(L) \approx \sum_{\mathbf{n}}[G''(\mathbf{R}-\mathbf{R}'+L\mathbf{n}) - G''(L\mathbf{n})]. \quad (36)$$

Now we turn to H_{ch2}. In order to get σ_α in terms of the charges we denote $\phi_{\alpha r}$ and q_R by $\phi_{\alpha ij}$ and q_{ij} where i and j (running from 1 to L) indicate the coordinates of a site r or of the lower left site of a plaquette R (cf. Fig. 3). We write σ_x in terms of differences on consecutive lines:

$$\sigma_x \equiv \sum_{ij}\phi_{xij} = \sum_{j=1}^{L-1} j\left(\sum_{i=1}^{L}\phi_{xij} - \sum_{i=1}^{L}\phi_{xij+1}\right) + L\left(\sum_{i=1}^{L}\phi_{xiL} - \sum_{i=1}^{L}\phi_{xi1}\right) + L\sum_{i=1}^{L}\phi_{xi1}. \quad (37)$$

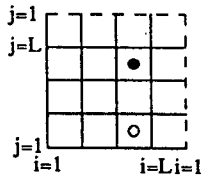

FIG. 3. Illustration of the coordinate system and of the notation. The full (or empty) circle indicates a positive (or negative) charge. It can be written $q_{33}=1$, $q_{31}=(1/2\pi)(\phi_{y31}+\phi_{x32}-\phi_{y41}-\phi_{x31})=-1$.

Then we use Eqs. (7) and (8) and choose the first horizontal line as the reference to define the topological charge $q_{x\alpha}$ [cf. Eq. (8)] associated with the periodic boundary conditions:

$$\sigma_x = -2\pi\left(\sum_{j=1}^{L} j\sum_{i=1}^{L} q_{ij} + Lq_{x1}\right). \quad (38)$$

In the same way in the other direction

$$\sigma_y = -2\pi\left(\sum_{i=1}^{L} i\sum_{j=1}^{L} q_{ij} + Lq_{y1}\right). \quad (39)$$

Since the system is neutral, the charges can be grouped by neutral pairs of unit charges. Considering each pair such that the positive charge is on a plaquette R_+ and the negative one on a plaquette R_-,

$$\sigma_x = -2\pi\left(\sum_{\text{pairs}}[j(R_+) - j(R_-)] + Lq_{x1}\right). \quad (40)$$

Now we define the suitable topological polarization vector $\mathbf{P}=(P_x, P_y)$ for the case of periodic boundary conditions in the θ_r's:

$$P_x \equiv \sum_{\text{pairs}}[i(R_+) - i(R_-)] + Lq_{y1},$$

$$P_y \equiv \sum_{\text{pairs}}[j(R_+) - j(R_-)] + Lq_{x1}. \quad (41)$$

So we have

$$\sigma_x = -2\pi P_y, \quad \sigma_y = -2\pi P_x, \quad (42)$$

and

$$H_{ch2} = 2\pi^2 J\left[\left(\frac{P_x}{L}\right)^2 + \left(\frac{P_y}{L}\right)^2\right]. \quad (43)$$

The above definition of the topological polarization removes the ambiguity of the polarization of a neutral pair of charges in a torus. The problem of the definition of the polarization of a Coulomb gas with periodic boundary conditions is well known. The problem arises as soon as a little pair is considered in the system: is it indeed a little pair or is it a very large pair comparable to the linear size of the lattice? However, the variables of the Coulomb gas associated with the wire model do not consist only of local charges, but also of two global charges corresponding to the periodic boundary conditions. And these additional charges permit one to define the polarization on a torus. Thus a definite neutral pair can correspond to different polarizations as it can correspond to a different topological configuration (not the same $q_{\alpha 1}$). For instance, the polarization of the pair in Fig. 4(a) is equal to $(1,3)$ whereas it is equal to $(1,-2)$ in Fig. 4(b).

Since $\mathbf{P}$ does not depend on the choice of the two reference lines defining the two $q_{\alpha 1}$'s, we can also define integer quantities q_{x0}, q_{y0}, $P_{\pi x}$, and $P_{\pi y}$ independent of

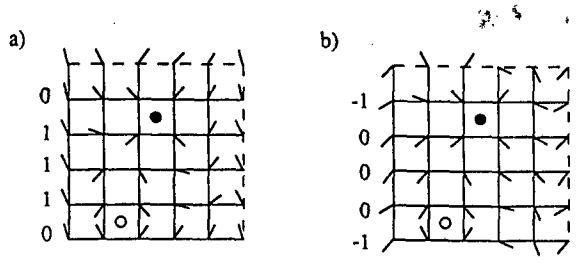

FIG. 4. Two configurations with same charges q_R, same q_{yi}'s (same $q_{y\alpha}$), and different q_{xj}'s (different $q_{x\alpha}$). (a) P=(1,3); (b) P=(1,−2). In this example, all the $\phi_{rr'}$'s are supposed to belong to $(-\pi,+\pi]$. The numbers on the left of each lattice are the values of the q_{xj}'s [cf. Eq. (8)].

reference choices using the following equations:

$$P_x = P_{\pi x} + Lq_{y0}\ , \quad P_y = P_{\pi y} + Lq_{x0}, \qquad (44)$$

where $P_{\pi x}$ and $P_{\pi y}$ are restricted to the interval $(-L/2,+L/2]$. Thus the $P_{\pi\alpha}$'s are the contributions of the charges q_R to the polarization $\mathbf{P}$ and the $q_{\alpha 0}$'s can be considered as the global topological charges associated with the torus topology. Another advantage of using $q_{\alpha 0}$ instead of $q_{\alpha 1}$ is that for a given set $\{q_R\}$ the Hamiltonian value is always minimum for $(q_{x0},q_{y0})=(0,0)$.

In order to understand the link of the wire model on a torus to a lattice Coulomb gas, we can use approximation (36) and write

$$H_{\rm ch} = -\frac{1}{2}\sum_{R\neq R'} q_{eR}q_{eR'}\left(\ln\mid \mathbf{R}-\mathbf{R}'\mid + \sum_{\mathbf{n}\neq 0}\left(\ln\mid \mathbf{R}-\mathbf{R}'+L\mathbf{n}\mid -\ln\mid L\mathbf{n}\mid\right)\right) + \sum_R q_{eR}^2\mu + \pi\frac{\mathbf{P}_e^2}{L^2} \qquad (45)$$

with $q_{eR} \equiv (2\pi J)^{1/2}q_R$, $\mathbf{P}_e \equiv (2\pi J)^{1/2}\mathbf{P}$, and $\mu \equiv (1/4)\ln 8 + \gamma/2$.

Thus the wire model with periodic boundary conditions in the θ_r's and $p_{rr'}$'s can be represented by a lattice Coulomb gas with the two additional variables q_{x0} and q_{y0} and a polarization energy. The topological charge q_R is represented by the number of electrical elementary charges on that plaquette. The two additional charges, and therefore the polarization, have no static electric meaning. However, in a dynamic case, they can be interpreted. Indeed, assuming that charges can only jump (and be created or annihilated by pairs) on nearest neighbor plaquettes, we could define an electric polarization variation between two electric charge configurations by summing elementary polarization variations. So the polarization would be defined by its variation from a reference state. In order to give such a polarization at an arbitrary time the positions of the charges would not be sufficient. We must in addition keep in memory the two $q_{\alpha 0}$'s which ensure that the polarization in Eq. (44) is indeed increased by elementary quantities. Those two variables can be interpreted as the difference between the total winding numbers of the positive charges and the negative ones around each direction of the torus.

Finally, the partition function of the wire model with periodic boundary conditions can be expressed exactly as the product of two factors:

$$Z = Z_{\rm SW}Z_{\rm ch}, \qquad (46)$$

with

$$Z_{\rm SW} = \int_{-\infty}^{\infty}[d\varphi_r]\exp\left(-\beta\frac{J}{2}\sum_{\langle rr'\rangle}(\varphi_r-\varphi_{r'})^2\right) \qquad (47)$$

and

$$Z_{\rm ch} = \sum_{\{q_R,q_{\alpha 0}\}}\exp\left\{-\beta 2\pi^2 J\left[\sum_{RR'}q_R G'_{RR'}q_{R'} + \left(\frac{\mathbf{P}}{L}\right)^2\right]\right\}, \qquad (48)$$

where the sum is taken over all topological configurations $\{q_R,q_{\alpha 0}\}$, and the q_R's and the $q_{\alpha 0}$'s can take any integer values subject to the constraint of neutrality, $\sum_R q_R=0$.

The first factor is the partition function of the spin waves representing the quadratic fluctuations around any equilibrium state and each of those states corresponds to a topological configuration. The second one can be represented by a neutral Coulomb gas on a lattice with two additional variables and a polarization energy. The topological charge q_R is exactly represented by the number of electric charges on the plaquette R. The polarization due to the two additional charges $q_{\alpha 0}$ could have an electrical meaning only in a dynamical version of the Coulomb gas.

An alternative way to map exactly the wire model onto a Coulomb gas without additional charges is to perform the sum over $q_{\alpha 0}$ in $Z_{\rm ch}$. But in that case we lose the possibility to represent completely the topology of a state by an electrical configuration.

A remark about fixed boundary conditions has to be made: in such a case, the Coulomb-gas Hamiltonian also contains an additional term involving the square of a polarization, but the boundary conditions and one set of q_R determine completely the polarization and the topology of a state.

B. Generalized XY model

We consider a generalized classical 2D XY model with Hamiltonian

$$H = \sum_{\langle rr'\rangle} V(\theta_r-\theta_{r'}), \qquad (49)$$

where V is a 2π-periodic, even, and continuous function. The site variables θ_r are restricted to the interval $(-\pi,\pi]$. The partition function is

$$Z = \int_{-\pi}^{\pi}[d\theta_r]\exp\left(\beta\sum_{\langle rr'\rangle}V(\theta_r-\theta_{r'})\right). \qquad (50)$$

Again it is useful to rewrite the Hamiltonian (49) in bond

variables $\phi_{rr'}$ defined as

$$\phi_{rr'} \equiv \theta_r - \theta_{r'} + 2\pi p_{rr'}, \tag{51}$$

where $p_{rr'}$ is the integer determined by $\theta_r - \theta_{r'}$ such that ϕ_{ar} belongs to the interval $(-\pi, \pi]$. (For a consistent definition of the $\phi_{rr'}$'s, it has to be noted that if r' is on the left hand side or below r, definition (51) implies $\phi_{rr'} \in [-\pi, \pi)$.) Then the Hamiltonian expressed in these variables becomes

$$H = \sum_{\langle rr' \rangle} V(\phi_{rr'}). \tag{52}$$

In order that Hamiltonians (49) and (52) agree, and for periodic boundary conditions in θ_r, the following constraints have to be imposed on each plaquette R:-

$$\sum_{\square R} \phi_{rr'} = 2\pi q_R \tag{53}$$

and

$$\sum_{r \in l_{a\alpha}} \phi_{ar} = -2\pi q_{a\alpha}. \tag{54}$$

As for the wire model, the quantity q_R represents the topological charge of the plaquette R and $q_{a\alpha}$ represents the global topological charge due to the periodic boundary conditions in direction α and is defined on an arbitrary line $l_{a\alpha}$ of the lattice. But, contrary to the wire model, the q_R's and $q_{a\alpha}$'s are not arbitrary integers since the ϕ_{ar}'s belong to the interval $(-\pi, \pi]$ and the topological charges must satisfy the inequality

$$\left| \sum_{R \in D} q_R \right| < \pi L_D \ , \quad \forall D \tag{55}$$

where the sum is taken over the plaquettes inside any domain D on the lattice and L_D is the perimeter of D. For instance, for the square lattice, the q_R's take values in the set $\{-1, 0, 1\}$. q_R=1 (−1) means that a vortex (antivortex) is centered in that particular plaquette.

For periodic boundary conditions, we have a one-to-one correspondence between each class of states $\{\theta_r\}$ (where two states are in the same class if they differ only by a same rotation of all spins) and each state $\{\phi_{rr'}\}$ satisfying the constraints (53) and (54). It is known that the XY model can be mapped onto a Coulomb gas[7] using Villain's approximation.[6] Actually, we shall see below that the mapping has not been done correctly for periodic boundary conditions in the original variables.

1. Villain's interaction

The interaction potential proposed by Villain[6] is

$$V_v(\Delta\theta) = -T \ln \sum_{n=-\infty}^{\infty} \exp\left(-\beta \frac{J_v}{2}(\Delta\theta + 2\pi n)^2\right) + c_v. \tag{56}$$

In order that V_v approximates some other given potential V, the parameter J_v has to be fitted for each temperature. This can be done by evaluating the value of $J_v = J_v(T)$ minimizing the mean quadratic difference on a period $(-\pi, \pi]$ of the two Gibbs factors, namely,

$$\exp[-\beta V(\Delta\theta) + \bar{c}],$$

and

$$\exp[-\beta V_v(\Delta\theta)] = \sum_{n=-\infty}^{\infty} \exp\left(-\beta \frac{J_v}{2}(\Delta\theta + 2\pi n)^2\right) + \bar{c}_v, \tag{57}$$

where $\bar{c}$ and $\bar{c}_v$ are normalization constants. In the limit of low temperatures, the potential V_v is a piecewise parabolic potential. For example, if we consider a potential $V(\Delta\theta)$ with an absolute minimum at $\Delta\theta = 0$ and such that the two first derivatives at $\Delta\theta = 0$ are $V'(0) = 0$ and $V''(0) > 0$, then J_v takes the value of $V''(0)$. On the other hand, in the limit of high temperatures V_v becomes a cosine function.

Replacing V by V_v in the partition function (50), we obtain

$$Z = \sum_{\{n_{rr'}\}} \int_{-\pi}^{\pi} [d\theta_r] \times \exp\left(-\beta \frac{J_v}{2} \sum_{\langle rr' \rangle} (\theta_r - \theta_{r'} + 2\pi n_{rr'})^2\right). \tag{58}$$

Therefore the partition function of the XY model with Villain's interaction potential and periodic boundary conditions is mathematically strictly identical to the one of the wire model in Eq. (9).

However, in this case the $n_{rr'}$'s are only independent summation variables, giving the potential V_v [see Eq. (56)], whereas a statistical configuration of the system is determined by the θ_r's. We have defined $\phi_{rr'}$, q_R, and $q_{a\alpha}$ with Eqs. (51), (53), and (54) for the XY model in order to give them a precise meaning in terms of the original variables. In order to apply the same calculations as done for the wire model, we have to introduce nonphysical variables $\tilde{\phi}_{rr'}$, $n_{rr'}$, m_R, and $m_{a\alpha}$ correspondingly to Eqs. (3), (6) and (8):

$$\tilde{\phi}_{rr'} = \theta_r - \theta_{r'} + 2\pi n_{rr'} \ , \quad m_R \equiv \sum_{\square R} n_{rr'} \ ,$$

$$m_{a\alpha} = -\sum_{r \in l_{a\alpha}} n_{ar}. \tag{59}$$

Thus Eqs. (46)–(48) are valid when replacing the q_R,q_{a0} by m_R,m_{a0} in these equations, as well as in expressions (38)–(41) for the polarization (replacing also q_{a1} by m_{a1}), but now the m_R's do not have the physical meaning of topological charges, in the same way as the φ_r in Eq. (47) would not have a precise meaning in the original variables. We cannot define a set of states $\{\theta_r\}$ corresponding to one configuration $\{m_R, m_{a0}\}$. However,

we shall see in Sec. III how to interpret the m_R's by expressing the correlation function $\langle m_R m_{R'}\rangle$ in terms of $\langle q_R q_{R'}\rangle$.

Our Coulomb gas, containing a polarization energy, does not correspond exactly to that of Ref. 7 where the authors performed the Coulomb-gas mapping in a different way, namely, by integrating the $\theta_{rr'}$ of the partition function Z. Noting that the contribution of a set $\{n_{rr'}\}$ is nonzero only if $\sum_{+r} n_{rr'} = 0$ for all sites r, they expressed the $n_{rr'}$'s by dual variables. But their definition of the dual variables was too restrictive in the case of periodic boundary conditions in the $\theta_{rr'}$'s. Indeed, they implicitly imposed the additional restrictions

$$\sum_r n_{\alpha r} = 0. \tag{60}$$

They would have obtained the same results as ours if they had taken this effect into account in the same way as given by our Eq. (18). On the other hand, we would have obtained the same charge Hamiltonian if we had taken the periodic boundary conditions only in the $\phi_{rr'}$'s instead of the $\theta_{rr'}$'s. However in this case the system would be decoupled into a spin-wave system, a Coulomb gas [described by Hamiltonian (28)], and two additional modes. The latter would correspond to Hamiltonian H_{ch2} [as in Eq. (21)], but being independent of the set $\{m_R\}$ and where σ_x and σ_y would characterize the states of the modes and take any real value.

2. *Piecewise parabolic interaction*

The piecewise parabolic potential is interesting because it permits one to map the XY model exactly onto a spin-wave system coupled to a Coulomb gas where the charges are indeed topological charges. This potential can be defined by

$$V(x) = \frac{J}{2}(x + 2\pi p)^2, \tag{61}$$

where p is the integer such that $x + 2\pi p \in (-\pi, \pi]$. Thus the Hamiltonian expressed in bond variables is the same as the one of the wire model (see Sec. II A):

$$H = \frac{J}{2}\sum_{\langle rr'\rangle} \phi_{rr'}^2. \tag{62}$$

Although the $\phi_{rr'}$'s are now restricted to the interval $(-\pi, \pi]$, the same computational steps used for the wire model Hamiltonian can be applied to treat the XY model with a piecewise interaction potential. Therefore, we can still split the Hamiltonian into two parts and express the part in the variables $\phi^0_{rr'}$ in terms of topological charge:

$$H = \frac{J}{2}\sum_{\langle rr'\rangle}(\varphi_r - \varphi_{r'})^2 + 2\pi^2 J \sum_{RR'} q_R G'_{RR'} q_{R'} + \frac{2\pi^2 J}{L^2}(P_x^2 + P_y^2). \tag{63}$$

However, the fluctuation part in the φ_r's is now no longer independent of the topological part (expressed by the q_R's) because for a given set of $\{q_R\}$ (corresponding to a set $\{\phi^0_{rr'}\}$) the φ_r's have to be such that each $\phi_{\alpha r}$ defined by Eq. (51) belongs to the interval $(-\pi, \pi]$. This fact expresses the coupling between the topological charges and the fluctuations around them. Thus two different interesting approximations can be applied in the case of the piecewise parabolic potential in order to map the system onto a Coulomb gas. The first one is to neglect the above coupling and to release the restriction on the q_R's (and $q_{\alpha a}$'s) thus yielding the same Coulomb gas as the wire model. The second one is to apply Villain's approximation, calculating first J_v as a function of J/T and then decoupling the partition function. The advantage of the first one is to give the possibility of interpreting directly the charges of the Coulomb gas as topological charges. However, the use of Villain's approximation yields a Coulomb gas mathematically identical to the one obtained using the first approximation but with a coupling constant J_v instead of J. As J_v is larger than J at any temperature (for this particular potential) we can interpret J_v/J as a correction related to the fact that the Coulomb-gas charges run through all integers instead of being restricted as topological charges are.

C. Frustration

In the frustrated case, the Hamiltonian for the wire model (1) becomes

$$H = \frac{J}{2}\int dl \left(\left|\frac{\partial \vec{S}_l}{\partial l}\right| + A_l\right)^2, \tag{64}$$

with $A_l = \vec{A}_l \cdot \hat{l}$ where $\vec{A}$ is a vectorial field (experimentally, $\vec{A}$ is proportional to a vector potential of a transverse magnetic field) and $\hat{l}$ is the unit vector oriented in the direction of the wire. So the partition function (9) becomes

$$Z = \sum_{\{p_{rr'}\}} \int_{-\infty}^{\infty} [d\theta_r] \exp\left(-\beta \frac{J}{2}\sum_{\langle rr'\rangle}(\theta_r - \theta_{r'} - A_{rr'} + 2\pi p_{rr'})^2\right) \tag{65}$$

with $A_{rr'} = \int_r^{r'} d\vec{l}\,\vec{A}_l$.

Now the bond variables have to be defined as

$$\phi_{rr'} = \theta_r - \theta_{r'} - A_{rr'} + 2\pi p_{rr'}, \tag{66}$$

and therefore satisfy the constraints

$$\sum_{\square R} \phi_{rr'} = 2\pi(q_R - f_R), \tag{67}$$

where $f_R = (1/2\pi)\sum_{\square R} A_{rr'}$ $[= -(1/2\pi)\oint_R d\vec{l}\cdot\vec{A}_l]$.

In the frustrated case the bond variables are particularly convenient since the system is now described in terms of gauge invariant quantities. So we are interested in periodic boundary conditions in gauge invariant variables and that periodicity implies the condition of "neu-

trality" for the frustrated case: $\sum_R(q_R - f_R)=0$. Then, if we impose in addition the periodicity in the θ_r's, we have to satisfy an additional constraint for each direction α:

$$\sum_{r\in l_{\alpha a}} \phi_{\alpha r} = -2\pi(q_{\alpha a} - f_{\alpha a}) \tag{68}$$

with

$$f_{\alpha a} \equiv -\frac{1}{2\pi}\sum_{r\in l_{\alpha a}} A_{\alpha r}, \tag{69}$$

where the sum is taken as in Eq. (8).

Two remarks are in order. First, it has to be noted that, in the case of boundary conditions in the θ_r's, the gauge invariance is restricted. Indeed, the system is invariant under a gauge transformation provided that the closed integral of the vector potential around each of the two directions of the torus is conserved. This condition on two arbitrary orthogonal lines is sufficient for it to be satisfied as well on all the other lines.

Second, no periodicity has been imposed in the $A_{rr'}$'s (otherwise the sum of the f_R's over the whole lattice could only be equal to 0). So the usual uniform frustrated case (f_R has the same value on every plaquette) can be considered. However, in order to satisfy the condition $\sum_R(q_R - f)=0$, the size of the lattice must be adapted to any particular uniform frustration. For example, it is never possible for an irrational uniform frustration to have periodic boundary conditions in the $\phi_{rr'}$'s.

After decoupling, we find

$$H = H_{\mathrm{SW}} + H_{\mathrm{ch}}, \tag{70}$$

with

$$H_{\mathrm{ch}} = 2\pi^2 J\left[\sum_{RR'}(q_R - f_R)G'_{RR'}(q_{R'} - f_{R'}) + \left(\frac{\mathrm{P}}{L}\right)^2\right] \tag{71}$$

and

$$P_x = \sum_{i=1}^{L} i\sum_{j=1}^{L}(q_{ij} - f_{ij}) + L(q_{y1} - f_{y1}), \tag{72}$$

$$P_y = \sum_{j=1}^{L} j\sum_{i=1}^{L}(q_{ij} - f_{ij}) + L(q_{x1} - f_{x1}). \tag{73}$$

As for the partition function the sum over $\{q_R, q_{\alpha 0}\}$ is taken over all configurations such that $\sum_R(q_R - f_R) = 0$.

For the frustrated XY model the Hamiltonian becomes

$$H = \sum_{\langle rr'\rangle} V(\theta_r - \theta_{r'} - A_{rr'}) \tag{74}$$

and the $\phi_{rr'}$'s are defined as in Eq. (66). But in this case the $p_{rr'}$'s will be determined by the θ_r's in order to include the $\phi_{\alpha r}$'s in the interval $(-\pi,\pi]$. For Villain's interaction the partition function is again identical to the one of the frustrated wire model, but after decoupling the m_R's (that replace the q_R's) are the circulations of the $\tilde{\phi}_{rr'}$'s defined as

$$\tilde{\phi}_{rr'} = \theta_r - \theta_{r'} - A_{rr'} + 2\pi n_{rr'}. \tag{75}$$

For the piecewise interaction potential the Hamiltonian can also be split in terms of q_R's and spin waves. The remarks about the gauge invariant property and the uniform frustrated case for the wire model hold for the XY model.

III. MEANING OF THE CHARGE IN THE COULOMB GAS ASSOCIATED WITH AN XY MODEL

For this purpose, we consider a frustrated XY model with a nonzero frustration only around two plaquettes R_1 and R_2 without common nearest neighbors (see Fig. 5). We could also perform the same following calculations for the frustrated case and they do not depend on the type of boundary conditions. The bond frustration terms around these two plaquettes (R_k with k=1 or 2), turning in the clockwise direction, are ε_k. Therefore the plaquette frustrations are

$$f_R = \begin{cases} 4\varepsilon_k/2\pi & \text{if } R = R_k, \\ -\varepsilon_k/2\pi & \text{if } R \text{ is nearest neighbor of } R_k, \\ 0 & \text{else.} \end{cases}$$

In order to see the physical meaning of the m_R, we shall calculate in the following the second derivative

$$\frac{\partial^2}{\partial\varepsilon_1\partial\varepsilon_2}\ln Z_\epsilon \tag{76}$$

in two ways: first in terms of the original variables θ_r and second in terms of the m_R's. Of course the second way becomes possible only after performing Villain's approximation, therefore it will be exact only in the case of Villain's interaction.

A. Partition function derivatives

Before distinguishing the two ways, expression (76) can be expressed in terms of thermodynamical averages:

$$\frac{\partial^2}{\partial\varepsilon_1\partial\varepsilon_2}\ln Z_\epsilon = -\beta\left\langle\frac{\partial^2 H}{\partial\varepsilon_1\partial\varepsilon_2}\right\rangle + \beta^2\left\langle\frac{\partial H}{\partial\varepsilon_1}\frac{\partial H}{\partial\varepsilon_2}\right\rangle - \beta^2\left\langle\frac{\partial H}{\partial\varepsilon_1}\right\rangle\left\langle\frac{\partial H}{\partial\varepsilon_2}\right\rangle. \tag{77}$$

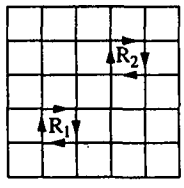

FIG. 5. The arrows indicate the frustrated bonds. $A_{rr'}=\varepsilon_k$ around R_k (k=1,2) and rr' is to be considered with the same orientation as the arrow. $A_{rr'}=0$ elsewhere.

Let us consider Hamiltonian (74) in terms of the $\phi_{rr'}$'s. The partial derivatives, evaluated at $\varepsilon_1 = \varepsilon_2 = 0$ are

$$\frac{\partial^2}{\partial\varepsilon_1\partial\varepsilon_2}\ln Z\Big|_{\varepsilon_1=\varepsilon_2=0} = \beta^2\left[\left\langle\left(\sum_{\square R_1}V'(\phi_{rr'})\right)\left(\sum_{\square R_2}V'(\phi_{rr'})\right)\right\rangle - \left\langle\sum_{\square R_1}V'(\phi_{rr'})\right\rangle\left\langle\sum_{\square R_2}V'(\phi_{rr'})\right\rangle\right]. \tag{78}$$

We shall call c_R the circulation of the derivative $V'(\phi_{rr'})$ around the plaquette R:

$$c_R \equiv \sum_{\square R} V'(\phi_{rr'}). \tag{79}$$

Now we note that the transformation $\theta_r \mapsto -\theta_r$ (or $\phi_{rr'} \mapsto -\phi_{rr'}$) on each node of the lattice does not change the Hamiltonian value (V is even by definition) but changes the sign of c_R. Thus we can write

$$\frac{\partial^2}{\partial\varepsilon_1\partial\varepsilon_2}\ln Z\Big|_{\varepsilon_1=\varepsilon_2=0} = \beta^2\langle c_{R_1}c_{R_2}\rangle. \tag{80}$$

Let us now perform the same derivation, but considering the charge Hamiltonian $H_{\rm ch1}$ in terms of the quantities m_R (the frustration does not contribute to the spin-wave part in the φ_r's and $H_{\rm ch2}$ is invariant under the ε transformation) as obtained after using Villain's approximation:

$$H_{\rm ch1} = 2\pi^2 J_v \sum_{RR'}(m_R - f_{\epsilon R})G'_{RR'}(m_{R'} - f_{\epsilon R'}), \tag{81}$$

where J_v=$J_v(T)$ depends on the considered interaction potential. We obtain

$$\frac{\partial^2}{\partial\varepsilon_1\varepsilon_2}\ln Z_\epsilon = -\beta J_v\left\langle\sum_{RR'}h_{1R}G'_{RR'}h_{2R'}\right\rangle + \beta^2(2\pi J_v)^2\left\langle\left(\sum_{RR'}h_{1R}G'_{RR'}(m_{R'} - f_{R'})\right)\left(\sum_{RR'}h_{2R'}G'_{RR'}(m_R - f_R)\right)\right\rangle$$
$$-\beta^2(2\pi J_v)^2\left\langle\sum_{RR'}h_{1R}G'_{RR'}(m_R - f_{R'})\right\rangle\left\langle\sum_{RR'}h_{2R}G'_{RR'}(m_R - f_{R'})\right\rangle, \tag{82}$$

where

$$h_{kR} = \begin{cases} 4 & \text{if } R = R_k, \\ -1 & \text{if } R \text{ is nearest neighbor of } R_k, \\ 0 & \text{else.} \end{cases}$$

The functions h_{kR} appear in the derivatives of $f_{\epsilon R}$ with respect to ε_k. Those functions correspond to the kth line of the matrix M, and therefore to those of the matrix $M_{c0} - c_0P$, and G' is by definition the inverse of M_{c0} (cf. Sec. II A). Furthermore, considering the neutrality property $\sum_R(q_R - f_R)$=0, the second variation at $\varepsilon_1 = \varepsilon_2 = 0$ becomes

$$\frac{\partial^2}{\partial\varepsilon_1\partial\varepsilon_2}\ln Z\Big|_{\varepsilon_1=\varepsilon_2=0}$$
$$= \beta^2(2\pi J_v)^2\left(\langle m_{R_1}m_{R_2}\rangle - \langle m_{R_1}\rangle\langle m_{R_2}\rangle\right). \tag{83}$$

Now we note that the transformation $m_R \mapsto -m_R$ on each plaquette of the lattice does not change the Hamiltonian value but changes the sign of m_R. From Eqs. (80) and (83), we are now able to write

$$\langle c_R c_{R'}\rangle \approx [2\pi J_v(T)]^2\langle m_R m_{R'}\rangle. \tag{84}$$

This relation becomes exact for Villain's interaction. We have shown that the quantities m_R and c_R are correlated in the same way. This gives us an interpretation to the m_R's. Therefore, the meaning of m_R depends on the interaction potential of the XY model. Thus, in Villain's approximation, the circulation c_R around a plaquette is composed of a quantized contribution and fluctuations around this quantized value which are treated as decoupled spin waves.

Note that experimentally in Josephson junction arrays (corresponding to the cosine interaction), the quantity c_R corresponds to the supercurrent circulation around a plaquette R where the site R is a lattice node located at the center of four superconducting grains.

B. Examples of interaction potentials

Now we can interpret the m_R's in terms of the q_R's for the XY model and end this section with three examples.

1. *Villain's interaction*

The interaction potential is

$$V(\phi) = -T\ln\sum_n \exp\left(-\beta\frac{J_v}{2}(\phi + 2\pi n)^2\right)$$

and the derivative becomes

$$V'(\phi) = \frac{J_v}{\sum_n \exp\left[-\beta\frac{J_v}{2}(\phi + 2\pi n)^2\right]} \times \sum_n\left[\exp\left(-\beta\frac{J_v}{2}(\phi + 2\pi n)^2\right)(\phi + 2\pi n)\right]. \tag{85}$$

We shall denote $\langle\cdots\rangle_\phi$ such an average over all integers n (not to be considered as a thermodynamical average). Thus by definition we have

$$V'(\phi) = J_v \langle \phi + 2\pi n \rangle_\phi \tag{86}$$

and

$$\sum_{\square R} V'(\phi_{rr'}) = J_v 2\pi \left(q_R + \sum_{\square R} \langle n \rangle_{\phi rr'} \right). \tag{87}$$

Comparing the charge-charge correlation functions in q_R and m_R we find

$$\left\langle \left(q_R + \sum_{\square R} \langle n \rangle_{\phi rr'} \right) \left(q_{R'} + \sum_{\square R'} \langle n \rangle_{\phi rr'} \right) \right\rangle \tag{88}$$

$$= \langle m_R m_{R'} \rangle. \tag{89}$$

2. *Piecewise parabolic interaction*

Since the variables $\phi_{\alpha r}$ are defined in the interval $(-\pi, \pi]$ we can simply write

$$V(\phi) = \frac{J}{2}\phi^2. \tag{90}$$

Therefore

$$V'(\phi) = J\phi \tag{91}$$

and we simply find

$$J^2 \langle q_R q_{R'} \rangle \approx [J_v(T)]^2 \langle m_R m_{R'} \rangle. \tag{92}$$

So for the piecewise parabolic potential, the result (83) leads to a direct identification of the m_R's with the topological charges q_R.

3. *Cosine interaction*

The cosine interaction potential is

$$V(\phi) = -J\cos(\phi). \tag{93}$$

We can define the function $X(\phi)$ in order to write

$$\sin(\phi) = \phi + X(\phi) \tag{94}$$

which yields

$$J^2 \left\langle \left(q_R + \sum_{\square R} X(\phi_{rr'}) \right) \left(q_{R'} + \sum_{\square R'} X(\phi_{rr'}) \right) \right\rangle \tag{95}$$

$$\approx J_v^2 \langle m_R m_{R'} \rangle. \tag{96}$$

IV. HELICITY MODULUS AND INVERSE DIELECTRIC CONSTANT

The helicity modulus Γ for a spin system with periodic boundary conditions in the angles of the spins expressing the "rigidity" of the system with respect to an applied "twist" equal to $L\delta$ between two opposite boundaries is given by Ref. 13:

$$\Gamma = \frac{1}{N} \frac{\partial^2 F}{\partial \delta^2}\bigg|_{\delta=0}. \tag{97}$$

Applying a twist implies that the periodic boundary conditions in the θ_r's in one direction have to be replaced by the condition that angles at opposite ends of the sample differ precisely by $L\delta$. Rather than changing the boundary conditions, it is, however, more convenient and strictly equivalent (it is simply a change of variables) to modify the frustration terms $A_{rr'}$ in the following way:

$$A'_{xr}(\delta) = A_{xr} + \delta\,, \quad A'_{yr}(\delta) = A_{yr}, \quad \forall r, \tag{98}$$

and to use again periodic boundary conditions. In fact, this corresponds to a gauge transformation leaving the frustration of all the plaquettes unchanged, but modifying the "frustration constraint" $f_{x\alpha}$ associated with the periodic boundary conditions.

Now the second derivative can be performed and expressed in terms of the thermodynamical average:

$$\Gamma = -\frac{T}{N}\frac{\partial^2}{\partial\delta^2} \ln Z$$
$$= \frac{1}{N}\left\{ \left\langle \frac{\partial^2 H}{\partial \delta^2} \right\rangle - \frac{1}{T}\left[\left\langle \left(\frac{\partial H}{\partial \delta} \right)^2 \right\rangle - \left\langle \frac{\partial H}{\partial \delta} \right\rangle^2 \right] \right\}. \tag{99}$$

In the nonfrustrated wire model or generalized XY model the term $\langle \partial H/\partial\delta \rangle^2$ vanishes at δ=0 because each state can be related to another one with the same energy and a derivative of opposite sign. In the frustrated case, we should adapt the gauge in order to fulfill the condition $\langle \partial H/\partial f \rangle = 0$ in $\delta = 0$. Thus we can write

$$\Gamma = \frac{1}{N}\left[\left\langle \frac{\partial^2 H}{\partial \delta^2}\bigg|_{\delta=0} \right\rangle - \frac{1}{T}\left\langle \left(\frac{\partial H}{\partial \delta}\bigg|_{\delta=0} \right)^2 \right\rangle \right]. \tag{100}$$

A. The wire model

Now we map the helicity modulus of the nonfrustrated wire model onto an inverse dielectric constant of a two-dimensional lattice Coulomb gas. The frustrated case could be treated in the same way. Since, in the charge representation, the frustration does not affect H_{SW} and the frustration variation δ does not change the f_R's, we can consider H_{ch2} instead of H in Eq. (100):

$$H_{ch2} = 2\pi^2 J \left[\left(\frac{P_x}{L} \right)^2 + \left(\frac{P_y}{L} \right)^2 \right], \tag{101}$$

where P_x and P_y are given by Eqs. (72) and (73) with $f_R = 0$, $f_{y1} = 0$, $f_{x1} = -L\delta/(2\pi)$, so that we have $P_y(\delta) = P_y(\delta = 0) + L^2\delta/(2\pi)$ and we can write

$$H_{ch2} = H_{ch2}(\delta = 0) + \delta 2\pi J P_y(\delta = 0) + \frac{J}{2}L^2\delta^2 \tag{102}$$

and

$$\Gamma = J\left(1 - \frac{4\pi^2 J}{TN}\langle P_y^2\rangle\right). \quad (103)$$

Since the two axis directions of the model are equivalent, we have $\langle P_x^2\rangle = \langle P_y^2\rangle$. And as we can find for any state of polarization (P_x, P_y) another one with the same energy and with a polarization $(P_x, -P_y)$, the quantity $\langle P_x P_y\rangle$ vanishes. Therefore, the helicity modulus becomes

$$\Gamma = J\left(1 - \frac{2\pi^2 J}{TN}\langle \mathbf{P}^2\rangle\right). \quad (104)$$

Now we can write $H_{\rm ch}$ and Γ in terms of a Coulomb gas in electric variables with an electric polarization $\mathbf{P}_e = e\mathbf{P}$ [$e = (2\pi J)^{1/2}$ is the elementary charge] and an external electric field $\mathbf{D} = (0, -e\delta)$:

$$H(\mathbf{D}) = H(\mathbf{D}=0) - \mathbf{D}\cdot\mathbf{P}_e(\mathbf{D}=0) + \frac{L^2}{4\pi}\mathbf{D}^2 \quad (105)$$

and

$$\Gamma = J\left(1 - \frac{\pi}{TN}\langle \mathbf{P}_e^2\rangle\right), \quad (106)$$

where $\mathbf{P}_e(\mathbf{D}=0)$ means [as in Eq. (102)] that $\mathbf{P}_e$ is defined with $f_{\alpha 1} = 0$.

Thus we can represent the twist δ in the direction x as an external electric field $\mathbf{D}$ that interacts linearly with the electric polarization $\mathbf{P}_e$. In order to establish the link between Γ and the dielectric constant ε, we define $1/\varepsilon$ as the response of the macroscopic electric field to a uniform external one:

$$\frac{1}{\varepsilon} \equiv \lim_{D_x\to 0}\frac{E_x}{D_x}. \quad (107)$$

By the use of the usual electrostatic relation

$$E_x = D_x - 2\pi\frac{\langle P_{ex}\rangle}{L^2}, \quad (108)$$

where P_{ex} corresponds to $P_{ex}(\mathbf{D}=0)$ as in Eq. (105) and expressing $\langle P_{ex}\rangle$ by the free energy derivative with respect to D_x,

$$\frac{1}{\varepsilon} = 1 - \frac{2\pi}{L^2}\lim_{D_x\to 0}\frac{\partial F/\partial D_x - \frac{L^2}{2\pi}D_x}{D_x} = \frac{2\pi}{L^2}\left.\frac{\partial^2 F}{\partial D_x^2}\right|_{D_x=0}. \quad (109)$$

Then the derivative is performed by Eq. (100) with Hamiltonian (105) and D_x replacing δ:

$$\frac{1}{\varepsilon} = 1 - \frac{2\pi}{TN}\langle P_{ex}^2\rangle = 1 - \frac{\pi}{TN}\langle \mathbf{P}_e^2\rangle. \quad (110)$$

Thus Γ/J is exactly represented by the dielectric constant of the associated Coulomb gas, $\Gamma/J = 1/\varepsilon$.

Furthermore, we can now correctly interpret our definition of the polarization in a dynamic Coulomb gas. When the charges are moving in an electric field, we have to take into account the winding number of the charges around the torus. Our definition of $\mathbf{P}$ corresponds then to the sum of the small displacements of the charges and therefore the term $-\mathbf{DP}$ is well represented by the coupling energy between the charges and the external electric field. But, in order to define such a displacement, we have to consider either a temporal succession of states (i.e., the dynamical version) or two additional fictitious variables that have no electric meaning in a static system.

Usually the susceptibility χ or the dielectric function ϵ of a Coulomb gas is defined in the Fourier representation. Then the dielectric constant is defined as the linear response to an oscillating field in the limit of large wavelengths. However, it has been known for a long time that in the usual Coulomb gas the linear response to a uniform electric field diverges ($\chi, \epsilon \to \infty$) in the thermodynamical limit (even at zero temperature) for periodic or free boundary conditions. The reason is that for an arbitrary nonzero electric field there always exists a finite distance of separation of the pairs beyond which the energy of the system decreases as their distance increases. This problem has been studied by Choquard, Piller, and Rentsch,[15] who considered various boundary conditions and showed that, even in cases where the susceptibility remains finite, it depends on the boundary conditions even at the thermodynamical limit. In our case at low temperature the response to a uniform external electric field remains finite because the additional polarization energy stabilizes the system. In the case of fixed boundary conditions, the wire model also has this additional polarization term but the definition of the polarization would not involve additional variables. For example, if we impose $\phi_{rr'} = 0$ on the boundary the charge representation would correspond to a Coulomb gas stabilized by the use of the image method (where a charge and its four images all have the same sign). In the case of free boundary conditions the system does not contain the additional polarization energy and the two additional variables are replaced by two additional modes [representing σ_x and σ_y as defined below Eq. (17) with Hamiltonian $H_{\rm ch2}$ (21)] which are independent of $H_{\rm SW}$ and $H_{\rm ch1}$ and take any real value.

Alternatively, in order to map the wire model on a Coulomb gas whose only variables are charges on the sites of the dual lattice we can integrate the partition function (48) over the $q_{\alpha 0}$'s and the mean square polarization appearing in Eq. (103), with P_α expressed as

$$P_\alpha = P_{\pi\alpha} + q_{\alpha 0}. \quad (111)$$

We find

$$Z_{\rm ch} = \sum_{\{q_R\}}\exp\left\{-\beta\left[H_{\rm ch1} + V_v\left(2\pi\frac{P_{\pi x}}{L}\right) + V_v\left(2\pi\frac{P_{\pi y}}{L}\right)\right]\right\}, \quad (112)$$

$$\Gamma = J\left[1 - \frac{2J}{T}\left\langle\frac{\partial}{\partial J}V_v\left(\frac{2\pi P_{\pi y}}{L}\right)\right\rangle\right]. \quad (113)$$

Here the occurrence of Villain's function is not due to an approximation. Thus we can also interpret $Z_{\rm ch}$ as the partition function of a Coulomb gas. In that case, the

twist would be represented by an external field with a nonlinear coupling to the polarization. Moreover, in this case an electric state $\{q_R\}$ represents a whole family of topological configurations.

B. Generalized XY model

In order to have a good understanding of the helicity modulus of the XY model in its Coulomb-gas representation, we can express it by performing the derivation of the Hamiltonian in Eq. (100) in the two representations. In terms of the variables $\phi_{rr'}$,

$$\Gamma = \frac{1}{N}\left[\left\langle \sum_r V''(\phi_{xr})\right\rangle - \frac{1}{T}\left\langle \left(\sum_r V'(\phi_{xr})\right)^2\right\rangle\right], \tag{114}$$

and in terms of the quantities m_R and $m_{\alpha 1}$, after the use of Villain's approximation:

$$\Gamma \approx J_v - \frac{1}{TN}\langle (2\pi J_v P_y)^2\rangle \tag{115}$$

with

$$P_y = \sum_{ij} j m_{ij} + L m_{x1}. \tag{116}$$

In both expressions for Γ the two quantities whose mean square is taken are the first derivatives $\partial H/\partial\delta$ at $\delta = 0$. Like this we can interpret the polarization in terms of the original variables.

Note that this interpretation is completely consistent with our results of Sec. III. Indeed, we could also express exactly the sum of the derivatives $V'(\phi_{xr})$ in Eq. (114) as a polarization of the circulations c_R [definition (79)] following the same computational steps [Eqs. (37) and (38)] as for the wire model. We obtain

$$\sum_r V'(\phi_{xr}) = \sum_{i,j} j c_{ij} + L c_{x1}, \tag{117}$$

where c_{ij} is the circulation of the current around a plaquette located by i and j. The quantity c_{x1} would be defined as the sum of the derivative $V'(\phi_{xr})$ over the horizontal reference line l_{x1}. After the use of Villain's approximation we can of course apply the results of Sec. IV A with the m_R's and $m_{\alpha 0}$ replacing the q_R's and the $q_{\alpha 0}$'s.

We conclude this section by discussing once more the three examples of interaction potentials.

For Villain's interaction the two expressions for Γ, given in Eqs. (114) and (115), are, of course, equal and Γ/J is exactly represented by an inverse dielectric constant even on a torus.

For the piecewise parabolic potential, we have to pay attention to a δ function appearing for $V''(\phi_{rr'})$ in Eq. (114), coming from the point where two parabolas in the potential join each other.

As for the cosine interaction, corresponding to Josephson junction arrays, the polarization represents the macroscopic current in the array and this current can also be expressed exactly as a "polarization" of elementary supercurrent loops.

V. CONCLUSION

We have studied the Coulomb-gas representation of the 2D XY model on a torus. We started from a phase field defined on a square wire network and with a Hamiltonian depending on the square gradient of the phase along the wire. After integrating the phase fluctuations between the nodes of the lattice, the partition function of this model becomes mathematically identical to the XY model with Villain's interaction. We mapped the wire model onto a lattice Coulomb gas defined on a torus. The charges of the Coulomb gas represent the topological charges of the wire model. The Coulomb gas contains an additional polarization energy where the polarization has been defined by the use of two additional integer variables. The latter come from the topological constraints expressing the periodic boundary conditions. Indeed, the topological charges corresponding to the plaquettes are not sufficient to define completely the topology of a given state of the system. The two additional variables allow us to define a polarization and, in a dynamic case, they correspond to the difference between the winding numbers of the positive charges and the negative ones around each direction of the torus. The twist δ allowing one to define the helicity modulus can be represented as an external uniform electric field, and therefore the helicity modulus is exactly related to the inverse of a dielectric constant. In the thermodynamic limit with a nonzero twist, the system is stable and the Coulomb gas with a nonzero electric field is also stable because of the additional polarization energy in the mapped Coulomb gas.

Alternatively we integrated the partition function over the two additional variables. Thus we obtained a Coulomb-gas representation whose charge configuration represents a family of topological configurations, and twist no longer corresponds to an external electric field coupling linearly with the charges of this Coulomb gas.

Since the wire model and the XY model with Villain's interaction possess a partition function with an identical structure, we can perform exactly the mapping for this particular XY model. But then the charges of the Coulomb gas do not represent the topological charges as defined in terms of the original variables.

We have derived expressions giving the meaning of the charges of the Coulomb gas associated with the XY model with Villain's interaction in terms of the original variables. For XY models with other potentials, the charges of the Coulomb gas obtained after performing Villain's approximation correspond to the circulations of the interaction potential derivatives around the plaquettes.

We have emphasized the case of the piecewise parabolic potential since it permits an exact splitting of the Hamiltonian into two independent terms: one expressing the topological charges and the other one the fluctuations around them. But the two subsystems are not really independent because the fluctuations have to belong to a

phase space determined by the topological configuration.

Our results apply as well for the frustrated models. We have performed our calculations with gauge invariant bond variables but on the torus this gauge invariance is restricted. Indeed, the usual gauge invariance is broken by periodic or fixed boundary conditions (imposed on the original variables).

Thus we have clarified the Coulomb gas representation of the 2D XY model on a torus. In particular we have expressed exactly the helicity modulus of the XY model with Villain's interaction in this representation. It becomes the inverse of a dielectric constant that we can define as the response of the internal electric field to an external uniform electric field. This will permit one to perform Monte Carlo simulations in a charge representation to evaluate the helicity modulus corresponding exactly to its definition in the spin variables.

ACKNOWLEDGMENTS

We are grateful to S. Korshunov, Ph. Choquard, J. Villain, J. M. Kosterlitz, and B. Grossmann for interesting discussions. This work was supported by the Swiss National Science Foundation.

[1] For a review, see *Coherence in Superconducting Networks*, Proceedings of the NATO Advanced Research Workshop, Delft, 1987, edited by J. E. Mooy and G. B. E. Schön [Physica B **152** (1988)].

[2] P. Martinoli, P. Lerch, C. Leemann, and H. Beck, Jpn. J. Appl. Phys. **26**, 1999 (1987).

[3] M. Rasolt, T. Edis, and Z. Tesanovic, Phys. Rev. Lett. **66**, 2927 (1991).

[4] M.P.A. Fisher, T.A. Tokuyasu, and A.P. Young, Phys. Rev. Lett. **66**, 2931 (1991).

[5] J.M. Kosterlitz and D.J. Thouless, J. Phys. C **6**, 1181 (1973).

[6] J. Villain, J. Phys. (Paris) **36**, 581 (1975).

[7] J.V. José, L.P. Kadanoff, S. Kirkpatrick, and D.R. Nelson, Phys. Rev. B **16**, 1217 (1977).

[8] M.E. Fisher, M.N. Barber, and D. Jasnow, Phys. Rev. A **8**, 1111 (1973).

[9] D.R. Nelson and J.M. Kosterlitz, Phys. Rev. Lett. **39**, 1201 (1977).

[10] R.J. Myerson, Phys. Rev. B **18**, 3204 (1978).

[11] P. Minnhagen and G.G. Warren, Phys. Rev. B **24**, 2526 (1981). For a review, see P. Minnhagen, Rev. Mod. Phys. **59**, 1001 (1987).

[12] T. Ohta and D. Jasnow, Phys. Rev. B **20**, 139 (1979).

[13] W.Y. Shih, C. Ebner, and D. Stroud, Phys. Rev. B **30**, 134 (1984).

[14] R. Savit, Phys. Rev. B **17**, 1340 (1978).

[15] P. Choquard, B. Piller, and R. Rentsch, J. Stat. Phys. **43**, 197 (1986); **46**, 599 (1987).

[16] F. Gallet and G.A. Williams, Phys. Rev. B **39**, 4673 (1989).

Frustrated XY models with accidental degeneracy of the ground state

S.E. Korshunov
L.D. Landau Institute for Theoretical Physics, Kosygina 2, 117940 Moscow, Russia

A. Vallat
Department of Physics, Brown University, Providence, Rhode Island, 02912

H. Beck
Institut de Physique, Université de Neuchâtel, Breguêt 1, CH-2000 Neuchâtel, Switzerland
(Received 23 September 1994)

The uniformly frustrated XY model on a triangular lattice is studied for two values of the frustration: $f = 1/4$ and $f = 1/3$. These two cases are very special because the ground states of the model have accidental degeneracy not related to symmetries. This degeneracy originates from the possibility of constructing domain walls with zero energy. At any finite temperature, the accidental degeneracy is removed by the spin-wave free energy, but the low free energy of the domain walls leads to the possibility of phase transitions at temperatures that are much lower than can be expected for the other values of the frustration not leading to accidental degeneracies. These conclusions are supported by Monte Carlo simulations. The results are of relevance for the description of Josephson-junction arrays in the presence of a perpendicular magnetic field.

I. INTRODUCTION

The progress made during the last decade in the experimental investigation of Josephson-junction arrays and superconducting wire networks has led to a revival of interest in various kinds of two-dimentional (2D) XY models which can be applied to the description of such superconducting systems.[1] Of particular interest is the uniformly frustrated XY model which describes regular Josephson-junction arrays in a perpendicular magnetic field. The Hamiltonian of this model can be written as

$$H = -\sum_{\langle \mathbf{r}\mathbf{r}' \rangle} \cos(\theta_{\mathbf{r}} - \theta_{\mathbf{r}'} - A_{\mathbf{r}\mathbf{r}'}), \qquad (1)$$

where the summation runs over pairs of nearest neighbors on some regular lattice. The Josephson coupling, the natural unit of energy in the system, has been set equal to 1. For each plaquette (i.e., site of the dual lattice) in a position $\mathbf{R}$ the restriction $\sum_{\Box\mathbf{R}} A_{\mathbf{r}\mathbf{r}'} = 2\pi f$ (where $\sum_{\Box\mathbf{R}}$ means the sum over the bonds surrounding the plaquette $\mathbf{R}$ in a clockwise direction) has to be obeyed. In terms of the Josephson-junction array the variable $\theta_{\mathbf{r}}$ corresponds to the phase of the $\mathbf{r}$th superconducting grain and f to the magnitude of the magnetic field expressed in the number of flux quanta per plaquette. Due to the symmetries of the cosine function Hamiltonian (1) is invariant with respect to the transformations $f \to f \pm 1$ and $f \to -f$, and so it is sufficient to study the interval $f \in [0, 1/2]$.

The main difference between ordinary (f=0) and frustrated XY models is that the ground state in the frustrated model has not only continuous but also descrete degeneracy. For example the f=1/2 model on square or triangular lattices has the Ising-type degeneracy associated with antiferromagnetic ordering of positive and negative vortices.[2] It was also discovered that, for f=1/2 on a hexagonal lattice and f=1/4 on a triangular one, different ground states can exist which are not related to each other by symmetry.[3–6] These ground states can be constructed from each other with the help of zero energy domain walls which are likely to have a strong influence on the properties of the system. The results of Monte Carlo simulations[3] do indeed indicate that both above mentioned cases as well as the f =1/3 (Ref. 5) model on a triangular lattice are characterized by a quite special behavior in comparison with all the other studied cases on these two lattices. Thus these particular systems seem to deserve more attentive consideration.

In the present paper we investigate the properties of the frustrated XY model on a triangular lattice with $f = 1/4$ and $f = 1/3$. Triangular arrays have also been investigated experimentally.[7] We will see that these systems—and in particular the case $f = 1/3$—present a wide family of ground states and zero energy domain walls which should give rise to rather special thermodynamic properties. We hope that our conclusions may also be of relevance for some other frustrated XY models.

II. VORTEX REPRESENTATION

Hamiltonian (1) depends on the choice of gauge variables $A_{\mathbf{r}\mathbf{r}'}$. The same model can be described in terms of gauge-invariant bond variables

$$\phi_{\mathbf{r}\mathbf{r}'} \equiv \theta_{\mathbf{r}} - \theta_{\mathbf{r}'} - A_{\mathbf{r}\mathbf{r}'} + 2\pi n_{\mathbf{r}\mathbf{r}'}, \qquad (2)$$

where $n_{\mathbf{r}\mathbf{r}'}$ is the integer for which the value of $\phi_{\mathbf{r}\mathbf{r}'}$ is shifted to the interval $(-\pi, \pi]$. These bond variables have to obey the constraints

$$\sum_{\square\mathbf{R}} \phi_{\mathbf{rr}'} = 2\pi(m_{\mathbf{R}} - f), \tag{3}$$

where $m_{\mathbf{R}} \equiv \sum_{\square\mathbf{R}} n_{\mathbf{rr}'}$ are the integers defined on the dual lattice. The $m_{\mathbf{R}}$'s should not be seen as additional independent variables: They are fully specified once the $\phi_{\mathbf{rr}'}$'s (belonging to a fixed interval of length 2π) are given and on a triangular lattice they can acquire only the values 1, 0 or -1. Hamiltonian (1) can be then rewritten in the form

$$H = -J \sum_{\langle \mathbf{rr} \rangle} \cos \phi_{\mathbf{rr}'},$$

subject to the constraints (3). The symmetries of different ground states can much more easily be recognized in terms of the gauge-invariant variables $\phi_{\mathbf{rr}'}$ (or $m_{\mathbf{R}}$) than in terms of the phase variables $\theta_{\mathbf{r}}$.

We can also define the quantitiy $Q_{\mathbf{R}} \equiv m_{\mathbf{R}} - f$ and interpret it as the topological charge on the corresponding plaquette. The total charge of any state will be equal to zero in the case of periodic boundary conditions. In the ground state the $Q_{\mathbf{R}}$ will acquire only the two different values $1 - f$ and $-f$ when $f \in (-\pi, \pi]$. This charge representation makes it possible to represent different locally stable states of the system (including all the ground states) by the corresponding configuration of the positive topological charges $1 - f$.

III. f=1/4

A. Ground states

For the case $f = 1/4$ the ground state that is depicted in Fig. 1(a) was the first to be discovered.[4] In the following we shall call it the hexagonal ground state. This ground state is characterized by a fourfold discrete degeneracy; i.e., by its translation along the lattice it is possible to obtain four nonequivalent states. It also has the continuous degeneracy associated with simultaneous rotation of all phases, which is not visualized in the charge representation.

The hexagonal state posesses a very interesting feature: For all bonds lying on straight lines that go through the centers of hexagons the gauge-invariant phase differences $\phi_{\mathbf{rr}'}$ are equal to zero. This allows one to construct domain walls with zero energy[6] by choosing one of these lines and shifting the configuration on one of its sides with respect to the other [Fig. 1(b)]. Doing this one obtains another ground state. Any of the three possible directions can be chosen for such a domain wall. However, in order to construct a ground state containing several zero energy domain walls, the latter should be all parallel to each other, because shifting the state along a $\phi_{\mathbf{rr}'}$=0 line breaks the $\phi_{\mathbf{rr}'}$=0 lines in the two other directions.

Nonetheless, an infinite number of states with the same energy can be constructed with the help of such zero energy domain walls. One of them is depicted in Fig. 1(c) (we shall call it the "necklace" ground state). It can be obtained from the hexagonal ground state by creating domain walls on all $\phi_{\mathbf{rr}'}$=0 lines going in the same direction. On the other hand the hexagonal ground state can equally be constructed from the necklace state by creation of an infinite number of zero energy domain walls.

It is well known that accidental degeneracies not related to lattice symmetries can be removed at arbitrary low temperatures due to differences in the spin-wave free energy.[8] So in order to understand what state will be dominant at low temperatures we should compare their spin-wave free energies.

B. Spin-wave free energy

In order to estimate the free energy of the system in the limit of low temperatures it is sufficient to consider the spin-waves in the harmonic approximation. Expanding Hamiltonian (1) up to second order in fluctuations around a ground state configuration $\{\bar{\phi}_{\mathbf{rr}'}\}$ one obtains

$$\begin{aligned} H &= -\sum_{\langle \mathbf{rr}' \rangle} \cos(\bar{\phi}_{\mathbf{rr}'} + \varphi_{\mathbf{r}} - \varphi_{\mathbf{r}'}) \\ &\approx \text{const} + \frac{1}{2} \sum_{\langle \mathbf{rr}' \rangle} K_{\mathbf{rr}'} (\varphi_{\mathbf{r}} - \varphi_{\mathbf{r}'})^2 \\ &\equiv \text{const} + \frac{1}{2} \sum_{\mathbf{rr}'} \varphi_{\mathbf{r}} M_{\mathbf{rr}'} \varphi_{\mathbf{r}'}, \end{aligned} \tag{4}$$

where $K_{\mathbf{rr}'} = J \cos \bar{\phi}_{\mathbf{rr}'}$ and M is the dimensionless dynamical matrix. The $\varphi_{\mathbf{r}}$'s are the deviations of $\theta_{\mathbf{r}}$ from the equilibrium values. The spin-wave free energy per site is given by

$$F_{\text{SW}} = -\frac{T}{N} \ln \sqrt{\frac{(2\pi)^N T^N}{\det M}}, \tag{5}$$

where N is the total number of the sites on the lattice. The zero eigenvalue of M which is related to the rotational invariance of (1) can be removed by fixing the sum of $\varphi_{\mathbf{r}}$ over the whole system.

For periodic ground states the position vector $\mathbf{r}$ can be decomposed into the sum $\mathbf{r} = \mathbf{u} + \mathbf{s}$, where $\mathbf{s}$ denotes the position of a site within an elementary cell of the ground state pattern located at $\mathbf{u}$. The harmonic Hamiltonian (4) can then be expressed in terms of plane waves:

$$H = \frac{1}{2} \sum_{\mathbf{q}ss'} \widetilde{\varphi}_{\mathbf{q}s} M_{ss'}(\mathbf{q}) \widetilde{\varphi}_{-\mathbf{q}s'}, \tag{6}$$

with

$$\widetilde{M}_{ss'}(\mathbf{q}) = \frac{1}{N} \sum_{\mathbf{uu}'} M_{\mathbf{u}+\mathbf{s},\mathbf{u}'+\mathbf{s}'} \exp\left[i\mathbf{q}(\mathbf{u} + \mathbf{s} - \mathbf{u}' - \mathbf{s}')\right]. \tag{7}$$

For example in the hexagonal ground state there are four inequivalent sites within the elementary cell, and so the matrix $\widetilde{M}_{ss'}(\mathbf{q})$ is 4×4. In the limit of a large system we get

$$F_{\mathrm{SW}} = \mu T - \frac{T}{2}\ln(2\pi T), \tag{8}$$

where

$$\mu \equiv \frac{1}{2}\int_{\mathrm{BZ}} \frac{d^2\mathbf{q}}{(2\pi)^2} \ln\det \widetilde{M}(\mathbf{q}). \tag{9}$$

We have calculated the coefficient μ numerically for five different ground states. In Table I the value of μ is reported as a function of a parameter ν expressing the concentration of the zero energy domain walls (all parallel to each other) on the background of the hexagonal ground state. Here $\nu=1/n$ means that the distance of two consecutive zero energy domain walls is equal to n times the distance between two nearest lines on the lattice; for instance $\nu=1/2$ corresponds to the necklace ground state.

It follows from Table I that the hexagonal ground state has the lowest free energy. It can be also seen that for the other ground states the difference in free energy with respect to the hexagonal one is almost exactly proportional to the concentration of the domain walls ν. One

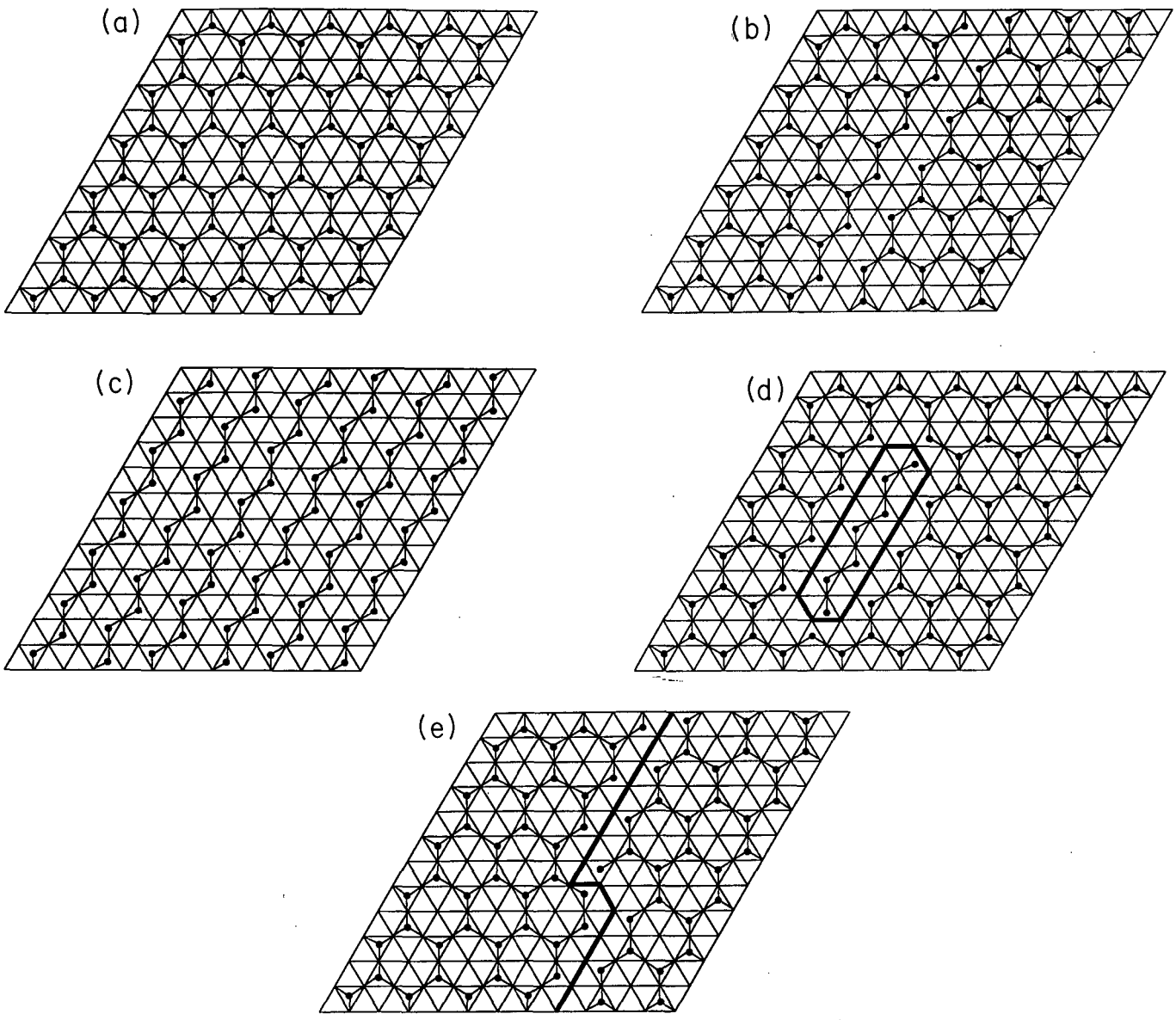

FIG. 1. $f=1/4$. (a) Hexagonal ground state. The values of the $\phi_{\mathbf{r}\mathbf{r}'}$'s are $\pi/2$ on the bonds surrounding a charged plaquette and 0 elsewhere. It is easy to spot the $\phi_{\mathbf{r}\mathbf{r}'}=0$ lines forming a triangular sublattice. The discrete degeneracy of that ground state equals 4. The segments linking the charges are guides to the eye in order to see easily the structure. (b) Ground state with a zero energy domain wall obtained by shifting one half plane of the hexagonal charge configuration along a $\phi_{\mathbf{r}\mathbf{r}'}=0$ line. (c) Necklace ground state obtained from the hexagonal ground state by introducing a maximum number of zero energy domain walls. (d) Low free energy defect or "strip" defect. There are two contributions to the free energy: One comes from the additional spin-wave free energy due to both zero energy domain walls and a second part from the nonzero energy of both defect end points. (e) Single kink. A defect as in Fig. 1(d) can be broadened by double kinks along a zero energy domain wall, but each kink involves an additional energy roughly equal to the one of a defect end point.

TABLE I. f=1/4. This table demonstrates the linearity of the spin-wave free energy as a function of the concentration of zero energy domain walls. Here 0 corresponds to the hexagonal ground state, 1/2 to the necklace ground state, and fractional values ν=1/n to the intermediate periodic ground states in which the distance between the domain walls is n times the distance between two nearest parallel lines on the lattice.

ν	μ	$\Delta\mu \equiv \mu - \mu(0)$	$\gamma \equiv \Delta\mu/\nu$
0	0.37527	0	–
1/8	0.37841	3.14×10^{-3}	2.512×10^{-2}
1/6	0.37948	4.21×10^{-3}	2.526×10^{-2}
1/4	0.38162	6.35×10^{-3}	2.540×10^{-2}
1/2	0.38774	12.47×10^{-3}	2.494×10^{-2}

can certainly interpret these results as evidence for the low interaction between the domain walls and can ascribe to a domain wall the finite free energy per unit length γT with $\gamma \approx 2.5 \times 10^{-2}$.

C. Low-temperature defects and phase transitions

Thus we have obtained that even the maximal difference in free energy for different ground states is very small and decreases with decreasing temperature. A natural question is whether this small difference may lead to any observable consequences. On the one hand a transition to a phase in which the ground state with the lowest spin-wave free energy will be dominant is possible. Alternatively a large concentration of defects leading to a mixture of different states could persist even at arbitrarily low temperatures. If such transition should really occur, at what temperature will it happen?

In order to investigate these questions we start our analysis from the hexagonal ground state which in the harmonic spin-wave approximation has the lowest free energy. This ground state, in addition to a fourfold discrete degeneracy, has also a continuous degeneracy, and so several different possibilities for the phase transitions are open, including the Berezinskii-Kosterlitz-Thouless vortex pair unbinding. At finite temperatures different types of defects on the background of the ground state will be thermally excited, but at low temperatures ($T \ll 1$) the vortices (corresponding either to adding or to substracting 1 to the $Q_{\mathbf{R}}$ of a plaquette from a ground state configuration) will be tightly bound in small pairs, and the energy of domain walls (with the exception of the special zero energy domain walls) will be too large for the corresponding defects to be excited. So the only extended defects that are expected to be present in the system at low temperatures will have the form of a strip enclosed by two zero energy domain walls [Fig. 1(d)].

The free energy of such a defect is equal to

$$F_D(L) = 2E + \alpha T L, \tag{10}$$

where L is the length of the strip (in units of the lattice constant),

$$\alpha = 2\gamma, \tag{11}$$

and $2E$ is the energy of the two end points of this defect. The defects with the minimal value of $E = E_0$ will dominate, and it seems very probable that E is minimal for the minimal distance between the zero energy domain walls [as in Fig. 1(d)]. A numerical evaluation of E_0 gives

$$E_0 \approx 0.44, \tag{12}$$

and the dependence on L would only lead to corrections smaller than 5×10^{-3}.

With the help of Eq. (10) it is easy to estimate the total concentration (per site) of such defects with any size L:

$$c = \frac{(3/m)\sum_{L=1}^{\infty} \exp[-F_D(L)/T]}{1 + (3/m)\sum_{L=1}^{\infty} \exp[-F_D(L)/T]}, \tag{13}$$

where m is the ratio of the total number of sites to the number of possible positions of the defect end points (for f=1/4 we have m=2). The factor of 3 comes from the summation over three possible directions. Performing the summation gives

$$c = \frac{1}{1 + \frac{m}{3}(e^{\alpha} - 1)\exp[2E_0/T]}, \tag{14}$$

and the average length $\langle L \rangle$ will be equal to

$$\langle L \rangle = \frac{1}{\alpha} + 1. \tag{15}$$

The defects will start touching or crossing each other for $c\langle L \rangle^2 \sim 1$. Since for f=1/4 we have $\alpha \approx 0.05$ and $\langle L \rangle \approx 21$ this will happen when the concentration c is much smaller than 1 and can be very well approximated by

$$c \approx \frac{3}{m\alpha} \exp[-2E_0/T]. \tag{16}$$

Comparison with Eq. (15) shows that for $\alpha \ll 1$ the relation $c\langle L \rangle^2 \sim 1$ will be fulfilled at temperatures close to

$$T_* = \frac{2E_0}{3 \ln \frac{1}{\alpha}}. \tag{17}$$

Since α is small, T_* is significantly smaller than 1, and therefore is substantially lower than the critical temperature observed in XY models having a similar rational frustration of the form f=p/q (with $q \leq 5$), but without an accidental degeneracy.

It has to be noted that concentration (14), based on Eq. (10), is evaluated by considering that the striped defects are independent of each other. Whenever two nonparallel defects are crossing each other, we should consider an additional energy that is roughly equal to $4E_0$, and so this effect makes the concentration (14) overestimated. On the other hand, adjacent parallel defects may have a lower free energy than if they were independent. To settle the question whether the latter effect is relevant we consider such a set of defects as a unique defect

but with kinks along its domain walls. Then we must compare the "bare" free energy of the domain wall to its decrease due to the presence of kinks [see Fig. 1(e)].

Let us consider a zero energy domain wall whose spin-wave free energy per unit length is equal to γT. Its free energy decrease due to configurational entropy of the kinks will be equal to

$$\Delta F = T \ln(1 + 2e^{-E_1/T}) \approx 2Te^{-E_1/T}, \qquad (18)$$

where E_1 is the energy of the kink. At a temperature $T_{**} \approx E_1/\ln\alpha^{-1}$, the total domain wall free energy $F_{\mathrm{DW}} = \gamma T - \Delta F$ becomes negative. In the vicinity of T_{**} both the number and the size of the defects should increase drastically due to the proliferation of the couples of kinks. So T_{**} yields an other interesting logarithmic estimate for a transition temperature.

We have found numerically that the value of E_1 differs from E_0 only by about 5×10^{-3}. So the direct calculation gives $T_{**} \approx (3/2)T_* > T_*$ and allows one to conclude that in the calculation of T_* the renormalization of α can be neglected. In addition, the comparison of the small difference between E_0 and E_1 with the additional energy due to a crossing of two defects implies that our concentration (14), based on independent simple striped defects, is overestimated. But at temperatures lower than T_* at which the defects are rare the above additional energy can also be neglected. Therefore the value of T_* given by Eq. (17) can be used as an estimate for the lower bound of a transition temperature, because there is no reason for a phase transition to take place when all defects are well localized and far from each other.

At temperatures higher than T_* the strip defects start merging with each other and the domain wall free energy rapidly tends to zero; so we have to expect the disappearance of the discrete order associated with the dominance of one of the four equivalent hexagonal ground states. This may happen as a first-order or a second-order phase transition. Since typical defects at low temperatures are very anisotropic and their crossing costs a relatively high energy one may think also of a possibility of the existence in some intermediate range of temperatures of the phase in which only noncrossing (i.e., parallel on the average) infinite domain walls are present. In this phase only two of the four possible hexagonal states will be intermixed (depending on the orientation of the infinite domain walls). Thus the transition associated with destruction of the discrete order may be split into two.

The other kind of ordering present in the system, that is, the XY-type ordering characterized by a finite rigidity (i.e., a finite helicity modulus), is not necessarily destroyed simultaneously with discrete ordering. From the structure of the zero energy domain walls it can be seen that they do not help to make a twist between two opposite sides of the system, and so the continuous degrees of freedom do not feel their presence directly and interact only with kinks and corners on the domain walls. The thermal fluctuations will lead to a decrease of the helicity modulus not only due to the presence of the strip defect end points and nonzero energy domain walls which affect locally the rigidity, but also due to presence of vortex pairs formed by the ordinary (integer) vortices or the fractional vortices which can be associated with corners on the domain walls.[6]

In the general situation the destruction of XY-type ordering is usually driven by the decoupling of (integer or fractional) vortex pairs, and the fractional vortices (if they can move around) are most dangerous since their interaction energy is the lowest.[6] In the present system, however, the fractional vortices are always linked by a domain wall with nonzero energy, and so in the vicinity of the temperature T_*, which is logarithmically small, all the effects leading to the decrease of the helicity modulus (including the presence of any kind of vortex pairs) can be expected to be not important. Therefore it looks more probable that the destruction of the XY-type ordering will take place as a separate phase transition at the temperature which is higher than T_*. It may be either a transition with a universal or higher than universal jump of the helicity modulus depending on what kind of vortex pairs will be dominant at the transition.

On the other hand it cannot be altogether excluded that the cumulative effect of all the mechanisms involved in the decrease of the helicity modulus in the vicinity of T_* (which is only logarithmically small) might be be sufficient to make that decrease important. In that case the simultaneous destruction of both types of ordering may happen which would be accompanied by a nonuniversal jump. One has to bear in mind, however, that in that case the destruction of the XY-type ordering may become observable only at the scales which are much larger than the typical size of the strip defect. In any case the presence of the large quantity of strip defects should lead to a significant decrease of the helicity modulus in comparison to the systems without accidental degeneracy.

IV. $f=\frac{1}{3}$

A. Ground states

The case of $f = 1/3$ demonstrates even a larger variety of ground states than $f=1/4$. One can again start from the ground state with hexagonal symmetry [Fig. 2(a)]. This is the one which is observed in Monte Carlo simulations and was recognized in Ref. 5. This state has a ninefold degeneracy. Just as in the case $f = 1/4$ the gauge-invariant phase differences $\phi_{\mathbf{rr}'}$ on the lines that go through the centers of hexagons are equal to zero, and so again the zero energy domain walls can be constructed [Fig. 2(b)]. However, in contrast to the case of $f=1/4$, a shift of a half plane of a ground state configuration along such a line can lead to two different configurations depending on the sign of the translation vector determining the shift [note the difference between the two zero energy domain walls in Fig. 2(b)]. As in the case of $f = 1/4$ it turns out to be possible to have an arbitrary number of such domain walls with the same orientation without any change in the total energy. If the domain walls are introduced on every possible position (and with the same direction of the shift), the ground state depicted

in Fig. 2(c) is obtained (the necklace ground state).

In all the ground states considered in this section the gauge-invariant bond variables $\phi_{\mathbf{r}\mathbf{r}'}$ are determined by the following rules:

(a) Each charged plaquette (i.e., the plaquette with $Q_{\mathbf{R}}=2/3$ or $m_{\mathbf{R}}=1$) is surrounded by three bonds on two of which $\phi_{\mathbf{r}\mathbf{r}'}$ (counted in clockwise direction) is equal to $\pi/3$ and on the third to $2\pi/3$.

(b) Each charged plaquette has three nearest neighbor plaquettes. Two of these have another charged plaquette

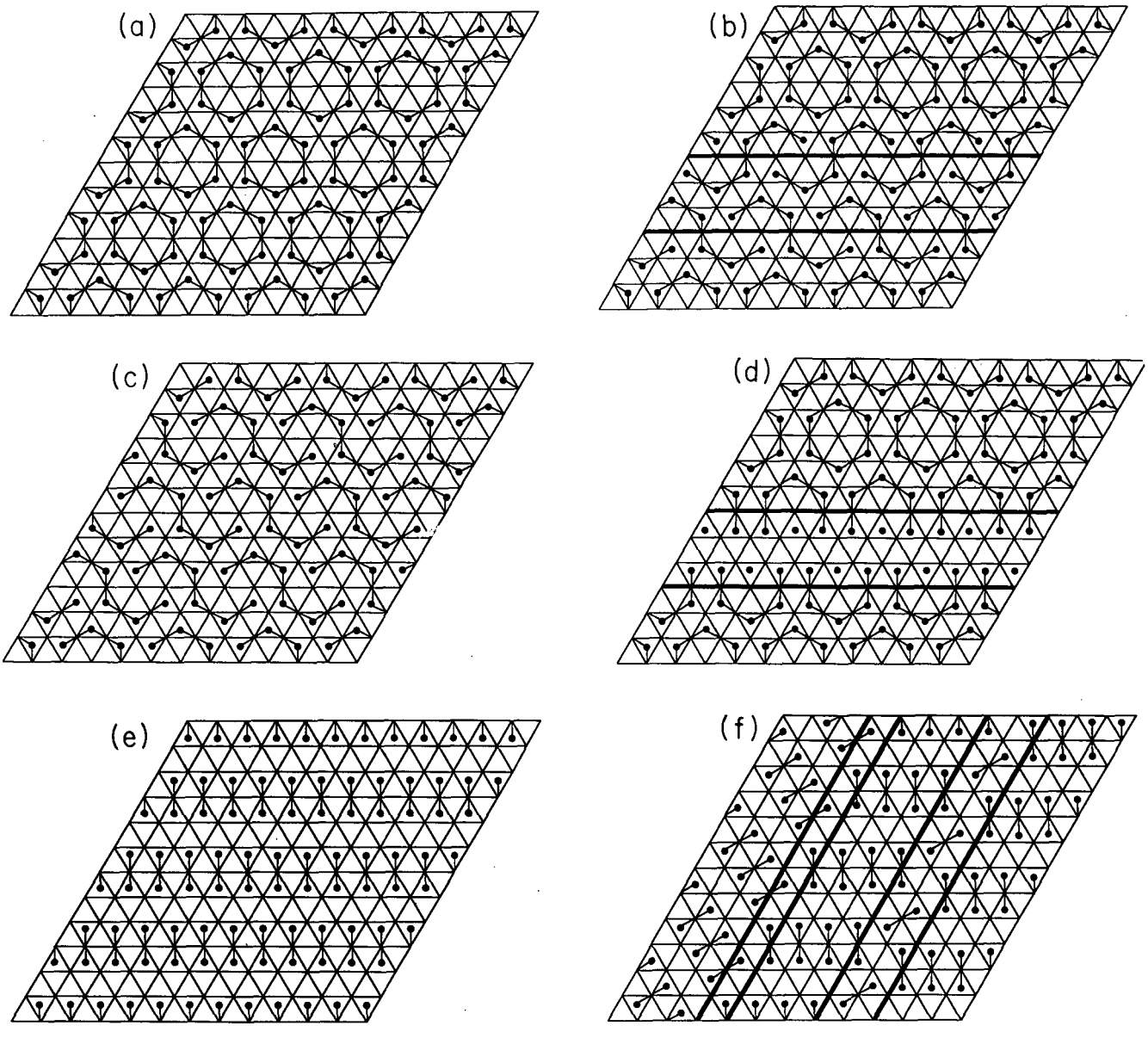

FIG. 2. $f=1/3$. (a) Hexagonal ground state. The $\phi_{\mathbf{r}\mathbf{r}'}$'s can be determined by the rules given in the text: the bonds carrying the value $2\pi/3$ form hexagons containing six noncharged plaquettes. The $\phi_{\mathbf{r}\mathbf{r}'}=0$ lines form a triangular sublattice the nodes of which are the centers of the hexagons. The partial discrete degeneracy of this ground state due to the lattice symmetry equals 9. (b) Ground state with two parallel zero energy domain walls along $\phi_{\mathbf{r}\mathbf{r}'}=0$ lines with different signs of the translation vector. The same hexagonal ground state lies above and below the zero energy defect. (c) Necklace ground state obtained from the hexagonal one with zero energy domain walls with the smallest possible distance and each one with the same sign for the corresponding translation vector. (d) Ground state with a strip consisting of a different configuration. As the horizontal $\phi_{\mathbf{r}\mathbf{r}'}=0$ lines are still there, it is still possible to perform shifts along them. Therefore we could also consider this strip as a thick zero energy domain wall. (e) Linear ground state obtained by repetition of the thick zero energy domain wall of (d). (f) Different linear ground states separated by zero energy domain walls not corresponding to $\phi_{\mathbf{r}\mathbf{r}'}=0$ lines. (g) Butterfly ground state obtained by a repetition of the wall depicted on the right hand side of (f). (h) Ground state with infinite size zero energy domain walls crossing one another. The horizontal domain walls correspond to those of (c). The vertical one corresponds to (d) but has been broken by the horizontal ones.

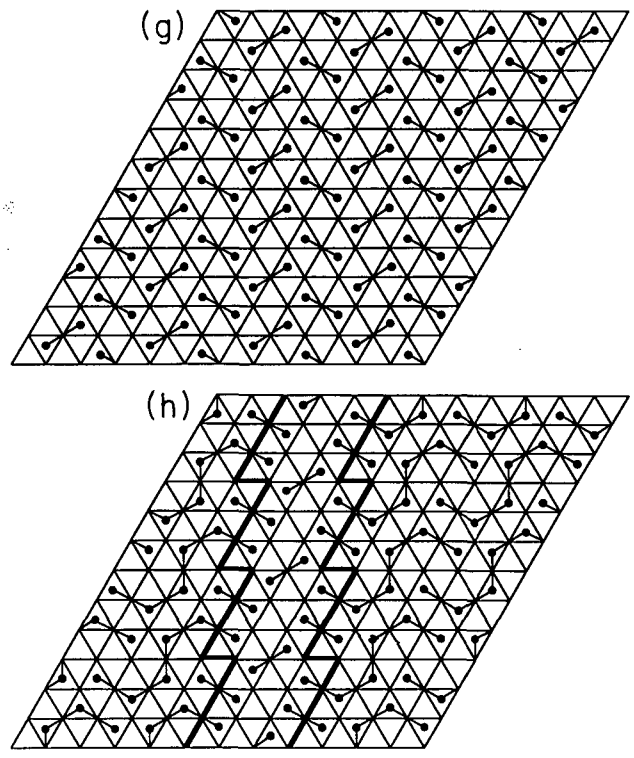

FIG. 2 *(Continued).*

as nearest neighbor, whereas the third does not. $\phi_{\mathbf{r}\mathbf{r}'}$ is equal to $2\pi/3$ on the bond which is ajacent to this particular plaquette.

(c) The bonds lying between uncharged plaquettes carry a zero value of ϕ.

The hexagonal ground state of the $f=1/3$ model allows also for the construction of zero energy domain walls with more complex structure [Fig. 2(d)]. Placing such strips one after another it is possible to construct the ground state with linear structure [Fig. 2(e)] that looks quite different from the hexagonal one. Of course different combinations of parallel strips of hexagonal, necklace, and linear ground states are also possible.

On the background of the linear ground state the zero energy domain walls can be constructed which are not related to $\phi_{\mathbf{r}\mathbf{r}'}=0$ lines [Fig. 2(f)]. Repeating such walls one after the other it is possible to construct one more periodic ground state ["butterfly" ground state, Fig. 2(g)] that again differs very much from all the states considered before. It is interesting to note that we have three different regular ground states (hexagonal, linear, and butterfly) which represent three different groups of planar symmetries.

It is also possible to construct ground states with infinite size zero energy domain walls crossing one another [Fig. 2(h)]. Indeed linear strips as in Fig. 2(d) in one direction and shifts as in Fig. 2(c) in another can be combined without change of energy. The example of Fig. 2(h) could be extended from the top of the figure by a hexagonal ground state with a nonbroken linear strip [as in Fig. 2(d) but with the strip in a different direction]. So there are many possible combinations, but the linear strips cannot be accompanied by any additional shift in the same direction and the shifts have to correspond to the same sign of the translation vector [as in Fig. 2(c)]. It is possible that other zero energy domain walls may exist. However, we have never found a ground state with zero energy defects of finite size.

B. Spin-wave free energy

We have calculated the spin-wave free energy for four different periodic ground states: hexagonal, necklace, linear, and butterfly. The coefficient μ in Eq. (9) is reported in Table II. As in the case of $f=1/4$ the hexagonal ground state (which, by the way, has the highest symmetry) turns out to have the lowest spin-wave free energy. This means that at low but finite temperatures this state will be dominant and the zero energy domain walls on its background will have a small but positive free energy.

As in the case of $f=1/4$ the extended defects with the lowest free energy have the form of strips enclosed by zero energy domain walls with finite energy defect end points. But now, starting from the hexagonal ground state, we can make such a defect not only by shifting the charges in the strip, but also by deplacing them to obtain the linear ground state inside the strip. We report in Table III the coefficient μ associated with periodic ground states constructed with a succession of such strips of infinite length. First we compare the hexagonal ground state with three different concentrations ν of domain walls: $\nu=0$ (corresponding to the hexagonal state), $\nu=1/6$ (corresponding to a shift on every sixth line), and $\nu=1/3$ (shift on every third line, which is the closest possible spacing). There are two results for $\nu=1/3$: The first (a) corresponds to the necklace state and the second (b) to shifts with regularly alternating directions [as in Fig. 2(b) but with a periodicity corresponding to six consecutive horizontal lines]. Finally, the two last results of Table III represent strips of the linear state (with periodicity corresponding to twice the strip width): The first corresponds to Fig. 2(d) and the second to a strip with the same hexagonal ground state below and above each strip [which is not the case in Fig. 2(d)].

From these results we conclude that the free energy associated with a $\phi_{\mathbf{r}\mathbf{r}'}=0$ domain wall separating two different hexagonal ground states is equal to $\gamma T \approx 6.3\times10^{-2}T$ per unit length. This gives $\alpha_s = 2\gamma \approx 0.125$ for the coefficient for a strip constructed by shifting. We will call such a strip a "shifted strip defect." We assume that the free energy will also be proportional to the concentration of strips of linear ground state. Thus we can ascribe a

TABLE II. $f=1/3$. Coefficient μ of the spin-wave free energy for four different types of ground state (g.s.)

g.s. type	μ	$\Delta\mu \equiv \mu - \mu(0)$
Hexagonal	0.23647	0
Necklace	0.25720	2.073×10^{-2}
Linear	0.26840	3.193×10^{-2}
Butterfly	0.33321	9.674×10^{-2}

TABLE III. f=1/3. ν is the fraction of the number of lines (in one direction) with a zero energy domain wall. This table shows the linearity of the spin-wave free energy as a function of the number of zero energy domain wall. The first value for ν=1/3 corresponds to shifts in the same direction and with the same orientation of the corresponding translation vectors, and the second to shifts with alternating opposite orientations. The two last lines correspond to periodic ground states with one linear strip every six lines. The second of them corresponds to an additional shift between the configuration of charge below and above the linear strip.

g.s. type	μ	$\Delta\mu$	γ
ν =0	0.23647	0	–
ν =1/6	0.24709	1.062×10^{-2}	6.372×10^{-2}
(a) ν =1/3	0.25720	2.073×10^{-2}	6.219×10^{-2}
(b) ν =1/3	0.25742	2.095×10^{-2}	6.285×10^{-2}
Linear strip	0.26607	2.960×10^{-2}	–
Linear strip+shift	0.26562	2.915×10^{-2}	–

value $\alpha_l = 6\Delta\mu \approx 0.18$ to the coefficient giving the free energy per length of a strip of linear ground state (the factor of 6 comes from the fact that there is one strip per six horizontal lines). We will call such a strip a linear strip defect. Comparing the two last results of Table III with the case of the uniform linear ground state in Table II we can decompose the free energy of a linear strip into two terms. The first of them can be associated with the "bulk" free energy of the linear state inside the strip and the second can be related to the boundaries between the two types of ground states.

C. Low-temperature defects and phase transitions

In contrast with the case of f=1/4 we now have to consider two kinds of extended defects at low temperature: the shifted strip defects [Fig. 2(b)] and the linear strip defects [Fig. 2(d)]. So we can calculate (numerically) the energies of the end points of each defect and estimate the characteristic temperatures in the same way as was done in Sec. III C but using a value of m equal to 4.5 (now the width of the strips is equal to 3 and their length can only be a multiple of 3/2). The results are shown in Table IV. We obtain that the characteristic temperature T_{*l} related to the linear strip defects is lower than T_{*s} related to the shifted strip defects. Thus although the lowest spin-wave free energy is for the defect of shifting type, the linear defects will be more numerous because of their lower defect end point energy.

TABLE IV. f=1/3. Characteristics of the two kinds of strip defects appearing at low temperature. The concentration c is calculated with Eq. (14). It can be noted that although α is not so small the approximation ($\alpha \ll 1$) we use to produce the definition of T_* [Eq. (17)] is not relevant according to the number of digits that are shown.

Defect	α	E_0	$\langle L\rangle$	T_*	$c(T=0.03)$	$c(T=0.1)$
Shift. strip	0.125	0.18	9	0.06	0.31×10^{-4}	0.12
Linear strip	0.18	0.086	6.5	0.03	1.08×10^{-2}	0.38

Nonetheless, the phase transition related to the disappearance of the discrete ordering should be associated with agglomeration and merging of shifted strip defects because only proliferation of these defects is equivalent to intermixing of different hexagonal states while linear strip defects correspond to the appearance of metastable states of the other type (involving an additional bulk free energy). Therefore we should use T_{*s} and not T_{*l} as an estimate for the transition temperature although such estimate would be less certain than for $f = 1/4$ due to the presence of the strip defects of the other type.

But as for f=1/4 we can still expect the hexagonal order to be destroyed at a logarithmically small temperature. It can be noted that the estimated temperatures are lower than for f=1/4 because of the lower defect end point energy. But even if the values of α are not so small, it is the zero energy domain walls that are responsible for the peculiar behavior leading to a temperature decrease of the phase transitions.

So the discussion of the different scenarios of the phase transitions that was made for f=1/4 in Sec. III C is also applicable for f=1/3. However, there may be two relevant differences between the two cases. First of all, the helicity modulus is likely to be more affected (at $T \sim T_{*s}$) due to the two kinds of low-temperature defects and thus the transitions may appear in a different sequence. Second, the type of discrete degeneracy associated with the hexagonal ground state is not the same for both cases; thus the transitions may be of a different nature.

Thus for both values of frustrations, the hexagonal order is destroyed at an unusually low temperature that depends on the spin-wave free energy of the zero energy domain walls. The latter are, furthermore, responsible for the lower temperature of the drop of the helicity modulus.

It is interesting to note that in contrast to the case of f=1/4, in the f =1/3 model the accidental degeneracy of the ground states will be removed if the form of the interaction is changed; that is, the higher harmonics are added to the interaction in Eq. (1). For example, in the superconducting wire network the effective interaction function at low temperature is very close to a piecewise parabolic function (with a periodicity of 2π). In that case the butterfly ground state of Fig. 2(g) will have the lowest energy. For $f = 1/4$ the accidental degeneracy cannot be removed by such a change of interactions.

V. MONTE CARLO SIMULATIONS

In this section we discuss some snapshots we have taken during Monte Carlo simulations and compare our predictions with what has been seen in simulations made by the other authors.

The striking feature of our shots (each from a 36 × 36 site system) is the disappearence of the hexagonal ordering at temperatures close to our estimates of T_* [cf. Figs. 3(a) and 3(c)]. Furthermore, the structure of the defects appearing at low temperature corresponds well to our analysis. In particular for f=1/3 at T=0.03 ($\approx T_{*l}$)

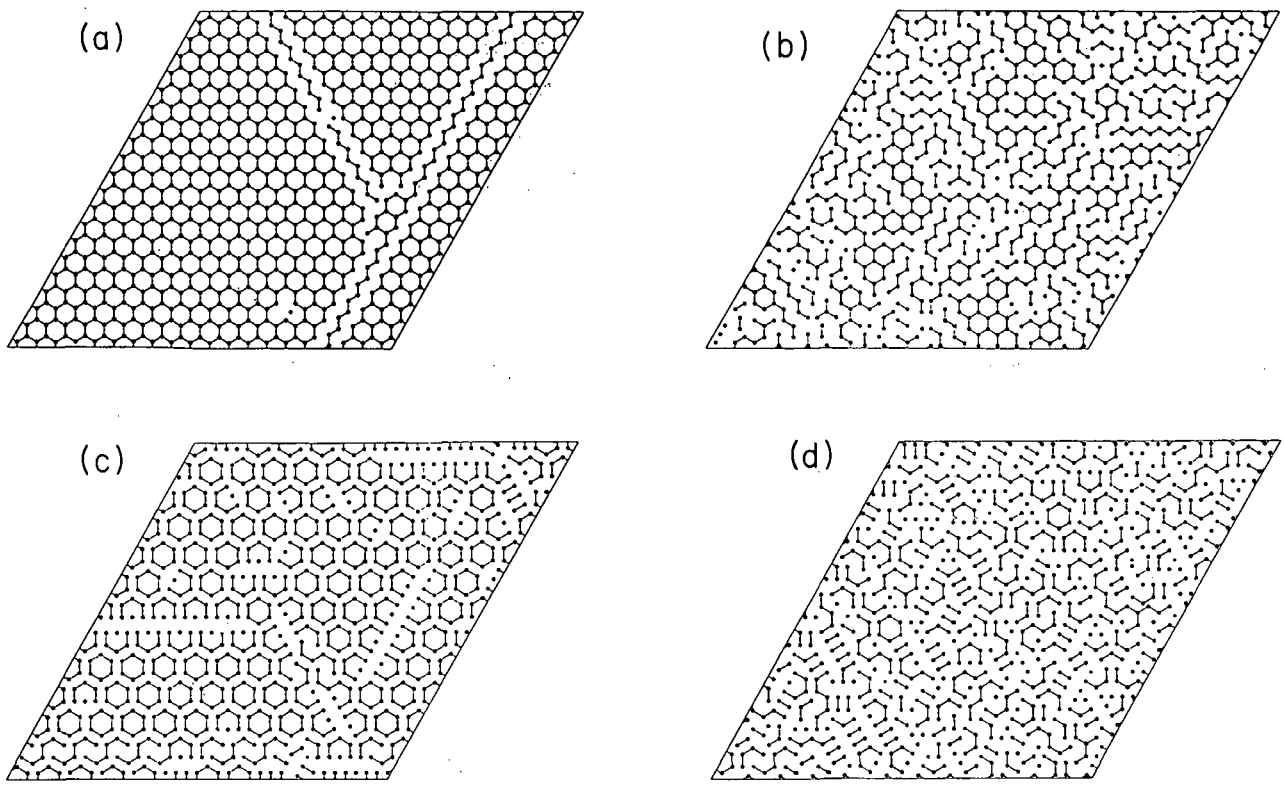

FIG. 3. $f=1/4$. (a) Snapshot at $T=0.1$ close to T_*. The segments linking the charges are a guide to the eye. We can spot two long defects. One of them runs through the whole lattice. The concentration c calculated with Eq. (14) is equal to 0.44×10^{-2}. (b) $f=1/4$. Snapshot at $T=0.25$ greater than T_*. The strip defects have broadened and we are not able to define clearly a main representative among the four hexagonal ground states. The concentration c calculated with Eq. (14) is equal to 0.46. (c) $f=1/3$. Snapshot at $T=0.03$ close to T_{*l}. We can mainly observe the presence of linear strip defects. Two shifted defects also occur but they are continued by linear ones which are likely to weaken the energy of their end points. (d) $f=1/3$. Snapshot at $T=0.1$ slightly greater than T_{*s}. Numerous defects are present and the hexagonal order is lost. We can also observe the rare occurrence of the butterfly ground state that would involve a higher spin-wave free energy.

mainly linear defects can be seen [Fig. 3(c)], whereas at $T=0.1$ both kinds of defects are present, although they cannot easily be distinguished because of their high density [cf. Fig. 3(d)].

Although the concentration c evaluated using Eq. (14) and quoted in the figure captions for $f=1/4$ and in Table IV for $f=1/3$ corresponds well to the shots observed close to T_* for both values of f, it is overestimated for higher T because the short-range interaction between the defects has not been taken into account. Obviously, the average length of the defects is equally overevaluated because we neglect the influence of the crossing energy of the defects. For $f=1/4$ we have found numerically that the crossing energy is twice the defect end point energy. For $f=1/3$, it depends on the particular type of defect crossing.

However, in several shots taken at low temperatures we have seen a strip defect going through the whole lattice [cf. Fig. 3(a)]. Such a defect has an abnormally low energy because of the lack of defect end points. This is a finite size effect that could deeply perturb the behavior of the system in the numerical simulations. Indeed such a defect has no energy dependence on the strip width (note that this is not true for the linear strip defect for $f=1/3$). So if the system size is not much larger than the typical size of the defects, the abnormal defect could take on too much statistical importance.

Finally, for both values of frustrations the hexagonal order seems clearly destroyed on the shots corresponding to a temperature larger than T_* in agreement with our predictions [see Fig. 3(b) for $f=1/4$ at $T = 0.25$, and see Fig. 3(d) for $f=1/3$ at $T=0.1$].

The Monte Carlo simulations on the triangular lattice made by Shih and Stroud[3] and by Kim, Lee, and Choi[9] (up to sizes of 256×256 for $f=1/4$) indicate that the phase transitions occur at an unusually low temperature for the frustrations $f=1/4$ and $f=1/3$. These temperatures correspond well to our analysis. Indeed for $f=1/4$ a maximum of the specific heat has been observed at $T \sim 0.15$ and this corresponds to the temperature of the proliferation of kinks we have estimated. The helicity modulus observed at this temperature seems to be larger than its critical value, but this is not conclusive because strong finite size effects are also observed even in large systems. Anyway, it drops at lower temperature than in any studied frustrated XY model without accidental de-

generacy. As for $f=1/3$, the helicity modulus drops at a temperature even lower than for $f=1/4$; this is as well in accordance with our conclusions.

Quite generally, it is rather difficult to study numerically the nature of the phase transitions in the XY model with accidental degeneracy because system sizes much larger than the typical size of the strip defect are needed to observe the destruction of the discrete ordering and still larger scales would be involved if one is interested in investigation of the mutual influence of two types of disordering. Therefore it may be rather difficult even to distinguish whether one single or two separate transitions take place.

VI. CONCLUSION

We have investigated the XY model on the triangular lattice for $f=1/4$ and $f=1/3$. Both values of the frustration manifest an infinite discrete degeneracy and a wide variety of the ground states which are related to each other not by the symmetries of the lattice but by the possibility of the construction of the special zero energy domain walls. This feature is the cause of the unexpected behavior which has been seen in numerical simulations.

At an arbitrarily small temperature the infinite degeneracy is removed by the spin-wave free energy, and in both cases studied the most favorable state is the one with the hexagonal symmetry (which is the highest degree of symmetry possible). The low free energy of the spin waves results in the unusual anisotropic form of the typical defects at low temperatures. Our low-temperature analysis allows us both to understand what low-temperature defects should be observed in numerical simulations and to obtain an estimate for the characteristic temperature below which nothing relevant should happen. At slightly higher temperature, but still small in comparison with critical temperatures for the other values of frustration (of the form $f=p/q$ with some small q) devoid of zero energy domain walls, both the hexagonal order associated with the discrete degeneracy of the hexagonal ground state and the XY quasi-long-range order are likely to be destroyed. However, we cannot draw any precise conclusions about the nature of the phase transitions. We have discussed various scenarios for the temperature behavior and pointed out some differences between $f=1/4$ and $f=1/3$ which could be relevant for the phase transitions of these systems.

Our analysis is supported by the results of Monte Carlo simulations. In the experimental situation the implications of the accidental degeneracy could be more difficult to observe because the details of the particular system can be important. As an example, the accidental degeneracy of the ground state can be removed by a small difference of the form of the phase-phase interaction (as happens for $f = 1/3$). Nevertheless, even if this degeneracy is removed, it is likely that an abnormal number of metastable states with low energy will persist, which could again be responsible for more numerous low-temperature excitations being possibly less mobile than other defects, since (around the critical temperatures) they would imply a more complex structure than usual. So it seems possible that a peculiar frequency behavior might be seen in dynamical measurements[10] on superconducting networks and arrays corresponding to an XY model with accidental degeneracy.

ACKNOWLEDGMENT

This work was supported by the Swiss National Science Foundation.

[1] For a review see *Proceedings of the NATO Advanced Research Workshop, Delft, 1987*, edited by J. E. Mooij and G. B. E. Schön [Physica B **152**, 1 (1988)].

[2] J. Villain, J. Phys C **10**, 4793 (1977); D. H. Lee, J. D. Joannopoulos, J. W. Negele, and D. P. Landau, Phys. Rev. Lett. **52**, 433 (1984).

[3] W. Y. Shih and D. Stroud, Phys. Rev. B **30**, 6774 (1984).

[4] M. Y. Choi and S. Doniach, Phys. Rev. B **31**, 4516 (1985).

[5] W. Y. Shih and D. Stroud, Phys. Rev. B **32**, 158 (1985).

[6] S. E. Korshunov, J. Stat. Phys. **43**, 17 (1986).

[7] R. K. Brown and J. C. Garland, Phys. Rev. B **33**, 7827 (1986); R. Théron, J. B. Simond, J. L. Gavilano, Ch. Leemann, and P. Martinoli, Physica B **165**, 1641 (1990); R. Théron, S. E. Korshunov, J. B. Simond, Ch. Leemann, and P. Martinoli, Phys. Rev. Lett. **72**, 562 (1994).

[8] H. Kawamura, J. Phys. Soc. Jpn. **53**, 2452 (1984); S. E. Korshunov, J. Phys. C **19**, 5927 (1986); C. L. Henley, J. Appl. Phys. **61**, 3962 (1987).

[9] S. Kim, S. Lee, and M. Y. Choi, Phys. Rev. B **46**, 1240 (1992).

[10] P. Martinoli, Ph. Lerch, Ch. Leemann, and H. Beck, Jpn. J. Appl. Phys. **26**, Suppl. 26-3, 1999 (1987); R. Théron, J. B. Simond, Ch. Leemann, H. Beck, P. Martinoli, and P. Minnhagen, Phys. Rev. Lett. **71**, 1246 (1993).